Organic & Biomolecular Chemistry

Accepted Manuscript

ROYAL SOCIETY OF CHEMISTRY

www.rsc.org/obc

Cite this: DOI: 10.1039/c0xx00000x

www.rsc.org/xxxxxx

ARTICLE TYPE

Pyrazole-oxadiazole Conjugates: Synthesis, Antiproliferative Activity and Inhibition of Tubulin Polymerization

Ahmed Kamal,[*a,d] Anver Basha Shaik,[a] Sowjanya Polepalli,[b] Vangala Santosh Reddy,[a] G. Bharath Kumar,[a] Soma Gupta,[a] K.V.S. Rama Krishna,[c] Ananthamurthy Nagabhushana,[d] Rakesh K Mishra,[d] Nishant Jain[b]

A number of pyrazole-oxadiazole conjugates were synthesized and evaluated for their ability to function as antiproliferative agents on various human cancer cell lines. These conjugates comprise of pyrazole and oxadiazole scaffolds closely attached to each other without any spacer as two structural classes. Type I class has a trimethoxy substituent and the type II class has 3,4-(methylenedioxy) substituent on their A rings. Among these conjugates **11a**, **11d** and **11f** manifest potent cytotoxicity with IC_{50} values ranging from 1.5 μM to 11.2 μM apart from inhibition of tubulin polymerization with the IC_{50} values 1.3μM, 3.9μM and 2.4μM respectively. Cell cycle assay showed that treatment with these conjugates result in accumulation of cells in G2/M phase and disrupt microtubule network. Elucidation of Zebrafish embryos revealed that the conjugates cause developmental defects. Molecular docking simulations determined the binding modes of these potent conjugates at the colchicine site of tubulin.

Introduction

In eukaryotic cells, the microtubules are hollow tubes of α- and β-tubulin heterodimers. The microtubule system is an important constituent of the cytoskeleton and microtubule functions in many fundamental cellular processes, including chromosome segregation during cell division, intracellular transport, development and maintenance of cell shape, cell motility and distribution of molecules on cell membranes.[1-4] In addition, microtubules are involved in a host of cell signaling pathways which are responsible for cellular apoptosis. The microtubule dynamics are regulated by various important proteins such as kinesin and dynein.[5-6] Many experiments have identified that microtubule dependence force underlying chromosomal translocation and spindle formation.[7] Hence altered/aberrant microtubule dynamics result in the obstruction of cell division, often at metaphase. As a result, various efforts aimed to block mitosis, like inhibition of tubulin polymerization by tubulin targeting agents has emerged as an attractive approach to cancer therapy.[8-9]

Microtubules possess three ligand-binding sites such as vinca, colchicine and taxol domains. Combretastatin A-4 (**1**) is one of the naturally occurring tubulin targeting agent that inhibits tubulin polymerization through the colchicine domain of the microtubule (Fig. 1A).[10] Among the common antitubulin agents, nocodazole (**3**) shows a preferential interference in the destabilization of microtubule polymerization (Fig. 1A).[11] Nevertheless, due to the incredible structural complexity of microtubule; inhibitors of tubulin exhibit tremendous diversity. This feature provides many possibilities for designing new molecular scaffolds and optimization to circumvent undesirable side effects like

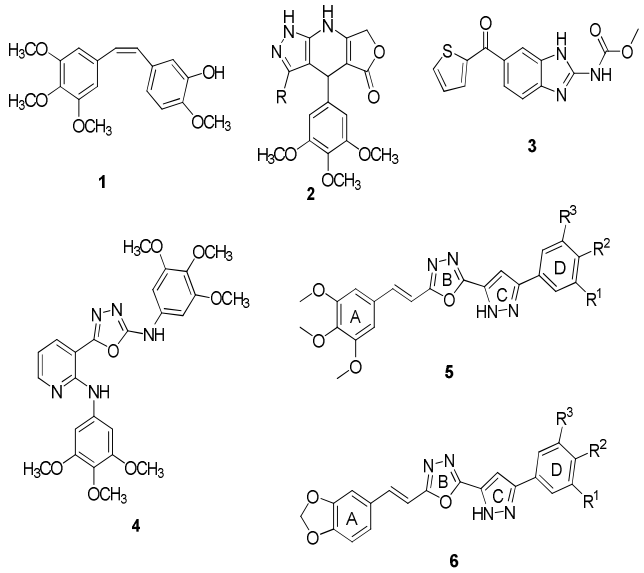

Fig. 1A Chemical structures of microtubule targeting agents: CA-4 (**1**), Azapodophyllotoxin (**2**), Nocodazole (**3**), Anilinonicotinyl-oxadiazole conjugate (**4**) and Pyrazole-oxadiazole conjugates (**5,6**)

reduced bioavailability, toxicity and multidrug-resistance.

Pyrazoles are wellknown representative compounds of potential importance for the design and development of anticancer agents that are considered as the building blocks in synthetic chemistry.[12-13] Moreover, some of the polysubstituted pyrazole derivatives showed a broad spectrum of antitumor potential towards most of the tumor cell lines.[14] Recently,

Magedov and coworkers performed biochemical studies on various dihydropyridopyrazoles (**2**) that inhibit tubulin polymerization to disrupt mitotic spindles (Fig. 1A).[15] Some tri- and tetra-substituted pyrazole derivatives exhibit impressive activity against Src, B-Raf wt, B-Raf V600E, EGFRs and VEGFR-2 thereby, making them as promising lead molecules for the development of chemotherapeutics.[16] Along with this, a number of oxadiazoles are familiar to display a wide range of biological activities including anticancer properties.[17-18] Recently, some 2,5-diaryl-1,3,4-oxadiazoline analogs of combretastatin A-4 (CA-4) were reported as potent microtubule disrupting agents and circumvent drug resistance mediated by P-glycoprotein and β-III tubulin expression.[19] In addition, some benzimidazole linked oxadiazole conjugates were reported to expresses significant anticancer effects.[20] More recently, few chemical entities that possess an oxadiazole group attached to hetero aromatic rings with an adjacent substituted amino functionality were documented as lead microtubule disrupting agents.[21] In this connection, we have also notice a report describing significant growth inhibitory activities of pyrazole incorporated oxadiazoles as potential antimicrobial agents.[22] Therefore, it was observed that, the combination of two heterocyclic moieties as a single molecular scaffold is known to enhance the anticancer activity.[23-24]

Previously we showed that incorporation of an oxadiazole ring system to a 2-anilinonicotinyl linked sulfonyl hydrazide scaffold (**4**) resulted in promising antitumor activity that significantly inhibit tubulin polymerization (Fig. 1A).[25a] Therefore, in our present endeavor to obtain potent anticancer agents through the combination of two pharmacophores, we designed and synthesized a new series of pyrazole-oxadiazole conjugates that comprise a scaffold of four rings (A, B, C and D). Consequently, for comprehensive analysis of structural activity relationships (SAR) by modifying A-ring, we synthesized two types of compounds. The type I class has a trimethoxy substituent on A ring, whereas the type II class has 3, 4-(methylenedioxy) as substituent on the A ring (Table 1). These pyrazole-oxadiazole conjugates were evaluated for their anticancer activity and ability to inhibit tubulin assembly. Out of the twenty conjugates three conjugates **11a, 11d** and **11f** showed pronounced anticancer a

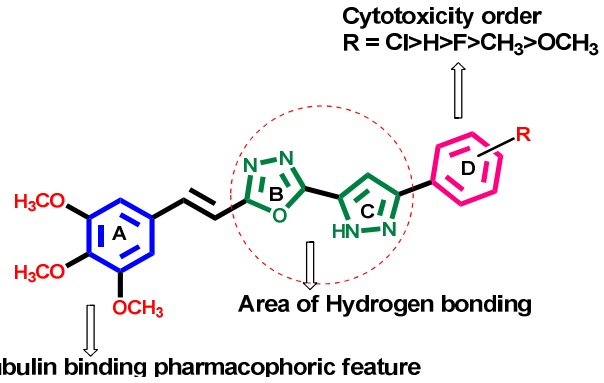

Fig. 1B SAR of type 1 pyrazole-oxadiazole conjugates.

Results and Discussion

Chemistry

Synthesis of pyrazole-oxadiazole conjugates **11a-i** and **12a-i** was successfully carried out by performing the reaction between 3-substituted phenyl-1H-pyrazole-5-carbohydrazides (**10a-i**) and 3,4,5-trimethoxy cinnamic acid/3,4-(methylenedioxy)cinnamic acid in the presence of $POCl_3$ as shown in Scheme 1.[25b] The crucial intermediates 3-substituted phenyl-1H-pyrazole-5-carbohydrazides (**10a-i**) were prepared conveniently in three sequential steps. Initially, different substituted acetophenones (**7a-i**) upon treatment with diethyl oxalate in the presence of sodium ethoxide afforded corresponding phenyl diketo esters (**8a-i**).[25c] Subsequently, these diketo esters underwent dehydrative cyclization with NH_2-NH_2.2HCl in refluxing ethanol to provide ethyl 3-substituted phenyl-1H-pyrazole-5-carboxylates (**9a-i**) in good yields.[25a] In the next step, these carboxylates (**9a-i**) were reacted with NH_2-NH_2.H_2O in ethanol to furnish 3-phenyl-1H-pyrazole-5-carbohydrazide (**10a-i**). Employing same synthetic procedures described above, the conjugates **17a-b** were synthesized starting with acetone (**13**) instead of substituted acetophenones as shown in the reaction sequence reported in Scheme 2. The desired target conjugates were characterized by IR, NMR and mass spectral data.

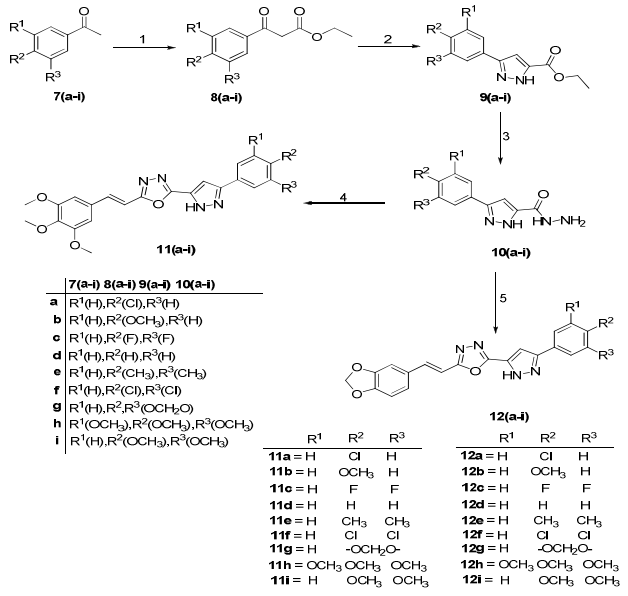

Scheme 1. Synthesis of pyrazole-oxadiazole conjugates (11a-i and 12a-i). *Reagents and conditions*: 1) NaOEt/Ethanol, diethyl oxalate, 0 °C-rt, 4 h; 2) N_2H_4.2HCl/ethanol, reflux, 3-4 h; 3) N_2H_4.H_2O/ethanol, reflux, 3-4 h; 4) 3,4,5-trimethoxy cinnamic acid, $POCl_3$, 110 °C 6 h; 5) 3,4-(methylenedioxy)cinnamic acid, $POCl_3$, 110 °C, 5 h

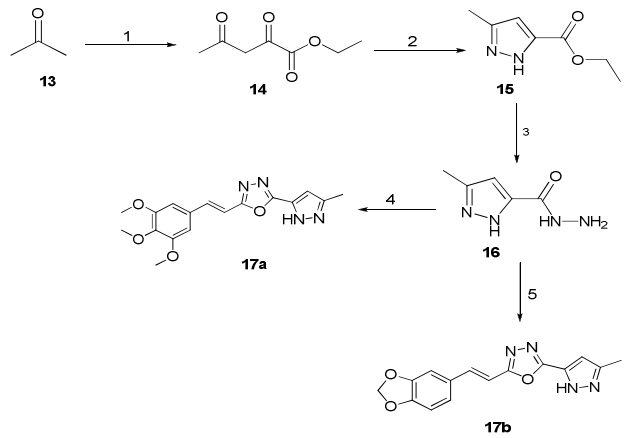

Scheme 2. Synthesis of pyrazole-oxadiazole conjugates (17a-b). *Reagents and conditions*: 1) NaOEt/Ethanol, diethyl oxalate, 0 °C-rt, 4 h; 2) N_2H_4.2HCl/ethanol, reflux, 3-4 h; 3) $N_2H_4.H_2O$/ethanol, reflux, 3-4 h; 4) 3,4,5-trimethoxy cinnamic acid, $POCl_3$, 110 °C 6 h; 5) 3,4-(methylenedioxy)cinnamic acid, $POCl_3$, 110 °C, 5 h

Table 1. Structures of pyrazole-oxadiazole conjugates **11a-i, 12a-i and 17a-b**

Structure	Compd	R^1	R^2	R^3	Mol.for	Mol.wt
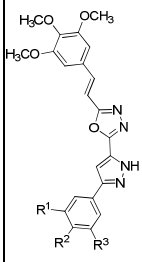	**11a**	H	Cl	H	$C_{22}H_{19}ClN_4O_4$	438.8
	11b	H	OCH_3	H	$C_{23}H_{22}N_4O_5$	434.4
	11c	H	F	F	$C_{22}H_{18}F_2N_4O_4$	440.4
	11d	H	H	H	$C_{22}H_{20}N_4O_4$	404.4
	11e	H	CH_3	CH_3	$C_{24}H_{24}N_4O_4$	432.4
	11f	H	Cl	Cl	$C_{22}H_{18}Cl_2N_4O_4$	473.3
	11g	H	-OCH_2O-		$C_{23}H_{20}N_4O_6$	448.4
	11h	OCH_3	OCH_3	OCH_3	$C_{25}H_{26}N_4O_7$	494.5
	11i	H	OCH_3	OCH_3	$C_{24}H_{24}N_4O_6$	464.4
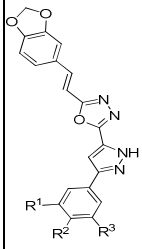	**12a**	H	Cl	H	$C_{20}H_{13}ClN_4O_3$	392.8
	12b	H	OCH_3	H	$C_{21}H_{16}N_4O_4$	388.3
	12c	H	F	F	$C_{20}H_{12}F_2N_4O_3$	394.3
	12d	H	H	H	$C_{20}H_{14}N_4O_3$	358.3
	12e	H	CH_3	CH_3	$C_{22}H_{18}N_4O_3$	386.4
	12f	H	Cl	Cl	$C_{20}H_{12}Cl_2N_4O_3$	427.2
	12g	H	-OCH_2O-		$C_{21}H_{14}N_4O_5$	402.3
	12h	OCH_3	OCH_3	OCH_3	$C_{23}H_{20}N_4O_6$	448.4
	12i	H	OCH_3	OCH_3	$C_{22}H_{18}N_4O_5$	418.4
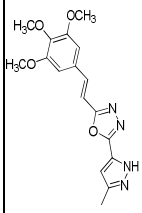	**17a**	-	-	-	$C_{17}H_{18}N_4O_4$	342.3
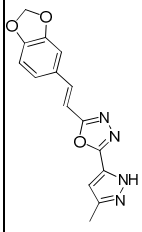	**17b**	-	-	-	$C_{15}H_{12}N_4O_3$	296.2

Biology

Antiproliferative activity

Initially, the pyrazole-oxadiazole conjugates were evaluated for their *in vitro* antiproliferative activity against a panel of four cancer cell lines such as HeLa, A549, MCF-7 and IMR32 employing sulphorhodamine B assay with nocodazole as reference standard. The IC_{50} values determined are summarized in Table 2. Majority of the conjugates significantly inhibit growth of the cells in a dose-dependent manner. The conjugates **11a-i** with trimethoxy substituents on A ring demonstrated better antiproliferative activity than **12a-i** that possessing a 3,4-(methylenedioxy) group on the same A ring (Fig. 1B). In detail, the conjugates with electronegative substituents i.e., -Cl and -F on D-ring expressed superior growth inhibition effect than electropositive (-OCH_3) groups on the same D-ring. Interestingly, type I class of conjugates **11a, 11d** and **11f** exhibit pronounced cytotoxicity towards all the cell lines with IC_{50} value ranging from 1.5μM-11.2μM. Specifically, the type I lead conjugate **11a** with a monochloro substitution at C4 position on the D-ring manifested significant inhibitory activity with an IC_{50} value of 1.5 μM in A549 cells. In comparison, **11d** is devoid of any substitution and **11f** with a dichloro at C3 and C4 (D-ring) showed an IC_{50} of 3.1 μM and 2.3 μM in A549 cells. In contrast, **11c** with difluoro substitution demonstrated moderate effects with an IC_{50} value 14 μM in A549 cells. Moreover, conjugate **11a** exhibited profound potency with an IC_{50} value of 1.8 μM in MCF-7; 2.3 μM in HeLa and 3.2 μM in IMR32 cell lines. However, the type II class of compounds of **12a-i** displayed moderate activities. Among these conjugates, substitution with monochloro- (**12a)** and dichloro- (**12f)** on the D-ring resulted an increased cytotoxicity against most of the cell lines. Further, conjugate **12d** devoid of any substitutions manifested an activity of 10 μM (IC_{50}) towards A549 cells. Notably, the presence of bulky groups on D-ring diminished the activities of the compounds in the type II class. Similarly, conjugates of type I class, such as **11h** harboring trimethoxy substitution at D-ring abrogated the potency of the conjugate. Based on these observations, removal of D-ring in **17a** and **17b** substantially reduced the potency, suggesting that the D-ring is essential for the optimal activity of these conjugates. Therefore, these results suggest that the trimethoxy group of the A-ring conjugated to chloro or un-substituted at C-4 position of D-ring are the most potent agents between the two structural classes of these conjugates.

Table 2. *In vitro* cytotoxic effect ([a]IC_{50} μM) of pyrazole-oxadiazole conjugates

entry	Compd	[b]A549	[c]Hela	[d]MCF-7	[e]IMR32
1	**11a**	1.5±0.1	2.3±0.5	1.8±0.3	3.2±0.6
2	**11b**	20±1.2	4.6±0.4	14.8±1.4	2.5±0.5
3	**11c**	14±2.1	17±1.5	21.8±0.8	14.8±1.4
4	**11d**	3.1±0.5	9.5±1.0	3.9±0.6	11.2±0.7
5	**11e**	13±1.4	16.2±1.0	21±1.9	17.9±1.3
6	**11f**	2.3±0.2	2.8±0.5	3.9±0.7	4.1±0.6
7	**11g**	20±1.6	32.3±2.5	11.2±1.0	24.3±1.4
8	**11h**	12±1.3	10±1.2	9.0±1.0	4.6±1.2
9	**11i**	21±1.5	19.4±1.7	19±2.1	16.7±1.8
10	**12a**	4.1±1.2	6.1±1.1	3.2±1.2	8.9±0.9
11	**12b**	33±1.5	10±1.2	16.2±2.1	20.9±1.8
12	**12c**	22±1.1	43.6±1.2	30±1.6	19.5±0.1
13	**12d**	10±1.7	12.0±1.6	11.0±1.8	7.6±1.2
14	**12e**	27±1.2	33.8±1.9	13±1.1	16.3±1.0
15	**12f**	13±0.6	15.0±1.0	8.9±1.7	14.5±1.2
16	**12g**	16±1.5	18.8±1.4	13±1.8	17.9±1.4
17	**12h**	12±1.1	18.2±1.2	23±1.7	21.4±1.2
18	**12i**	24±1.6	12.0±1.2	14.1±1.6	19.1±0.6
19	**17a**	19±1.0	9.3±1.8	19.2±0.9	19±1.0
20	**17b**	23±1.5	18.7±1.0	15.5±1.8	12.9±1.0
21	**Noc**	0.9±0.2	1.2±0.7	1.25±0.9	1.3±0.7

[a] Concentration required to inhibition 50% cell growth and the values represent mean ± S.D. from three different experiments performed in triplicates. [b] A549: lung adenocarcinoma epithelial cell line. [c] HeLa: cervix cancer cell line [d] MCF-7: breast adenocarcinoma cell line. [e] IMR32: Neuroblastoma cell line.

Dot-blot analysis for Cyclin-B1

Previously our studies showed that 2-anilino-nicotinyl 1,3,4-oxadiazoles, with a trimethoxy phenyl group, oxadiazole and pyridine moiety function as potent anti-tubulin agents.

Therefore, we hypothesize that these conjugates induce cytotoxicity through cell cycle arrest at G2/M phase. Accumulation of cyclin-B1 is an indicator for G2/M arrest[26]. Hence, we treated A549 cells with all the conjugates at 5 µM concentrations for a duration of 24 h and performed dot-blot analysis for cyclin-B1. Interestingly, **11a** and **11f** exhibited a marked increase in cyclin-B1 protein levels similar to colchicine and CA-4 treated cells. In addition, **11d, 11g, 11h** showed slight increase in cyclin-B1 protein. Therefore, these results support the suggestion that congeners, **11a, 11f** of pyrazole-oxadiazole conjugates manifest anti-proliferative effects through cell cycle arrest at mitosis (Fig. 2).

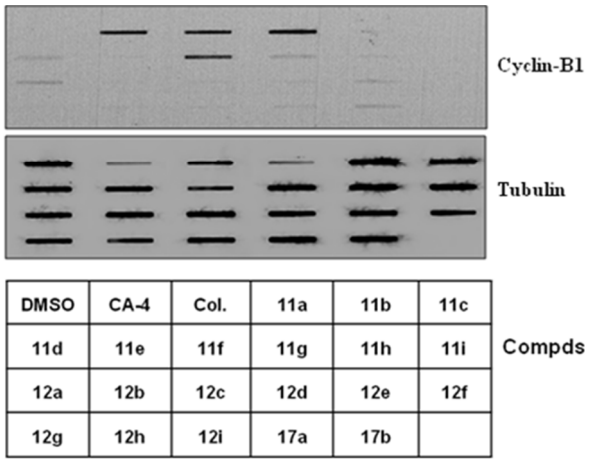

Fig. 2 Dot-blot analysis of Cyclin-B1: A549 cells were treated with 5 µM concentrations of pyrazole-oxadiazole conjugates for 24 h. Later, cells were harvested and whole cell lysates were blotted on nitrocellulose membranes. The blotted proteins were probed with antibodies against, Cyclin B1. Tubulin was employed as loading control.

Effect on tubulin polymerization

Since conjugates of type I class of compounds harbor trimethoxy phenyl, oxadiazole and pyrazole moiety, we presumed that these conjugates can prevent tubulin assembly. Based on our SAR analysis and dot-blot results we selected that **11a** and **11f** as potent congeners. Intriguingly, though **11d** treated cell showed modest increase in cyclin B1 protein levels. In contrast, **11d** exhibited potent cytotoxicity compared to the other conjugates in the series. Consequently, we elucidated the ability of **11a, 11d** and **11f** to inhibit tubulin assembly. Thus, we incubated varying concentrations of the lead conjugates with tubulin to determine the IC_{50} values for inhibition of tubulin polymerization. As expected, **11a**, which potentially inhibited cell growth also significantly down regulated tubulin polymerization with an IC_{50} value 1.3 µM when compared to **11d** and **11f**. However, **11d** and **11f** also inhibited tubulin assembly at an IC_{50} value 3.9 µM and 2.41 µM respectively (Table 2 and Fig. 3).

Effect on cell cycle arrest

Anti-microtubule agents are known to induce cell cycle arrest in the G2/M phase of cell cycle. Flow cytometry is routinely employed to determine the population of cells in each phase of the cell cycle by measuring the DNA content of individual cells. Since conjuagtes **11a**, **11d** and **11f** bind tubulin and inhibit cell gowth, we analyzed for their ability to arrest cells at G2/M phase. Therefore, A549 cells were treated with 5 µM concenterations of representative compounds for 24h. Subsequently, harvested cells were subjected to flow cytometry analysis. The lead conjugate **11a** showed an increase of cells in G2/M phase to 77.3%. In comparsion, cells accumlated to 75.02% and 75.07% in **11d** and **11f** treatments in G2/M phase. Moreover, cell number significantly decreased in the S phase. In contrast, vehicle or DMSO treated cells showed a majority of the population in G1 phase (67.7%) and **11a**, **11d** and **11f** treated cells resulted in a significant increase of cyclin-B1 protein, compared to DMSO treated cells (Fig. 4). Thus treatment with the pyrazole-oxadiazole conjugates resulted in a clear G2/M arrest with a concomitant decrease of cells in other phases of cell cycle and induction of cyclin-B1 protein.[27]

Table 2 Antitubulin Activity of pyrazole-oxadiazole conjugates **11a, 11d** and **11f** values expressed in IC_{50} (µM)

Compound	Inhibition of Tubulin polymerization (µM)
11a	**1.3 ± 0.1**
11d	**3.9 ± 0.05**
11f	**2.41 ± 0.32**
CA4	**0.91 ±0.01**

Effect of conjugates on tubulin polymerization. IC_{50} values for **11a, 11d** and **11f** were determined from the tubulin polymerization assays.

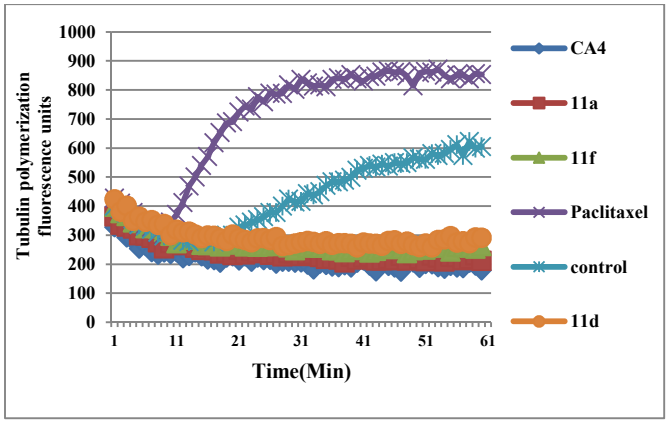

Fig. 3 Effect of lead conjugates 11a, 11d and 11f on tubulin polymerization: Tubulin polymerization was monitored by the increase in fluorescence at 360 nm (excitation) and 420 nm (emission) for 1 h at 37^0C. All the compounds were included at a final concentration of 5µM. Combretastatin A-4 (CA-4) and Paclitaxel were used as a positive controls.

Effect on microtubule network

Spindle poisons exert their action through the disruption of chromosome separation during mitosis. The pyrazole-oxadiazole conjugates significantly decreased cell growth, inhibited tubulin assembly and stalled cells in G2/M phase of cell cycle. Therefore, we evaluated their ability to disrupt microtubule network in cells. Consequently, A549 cells

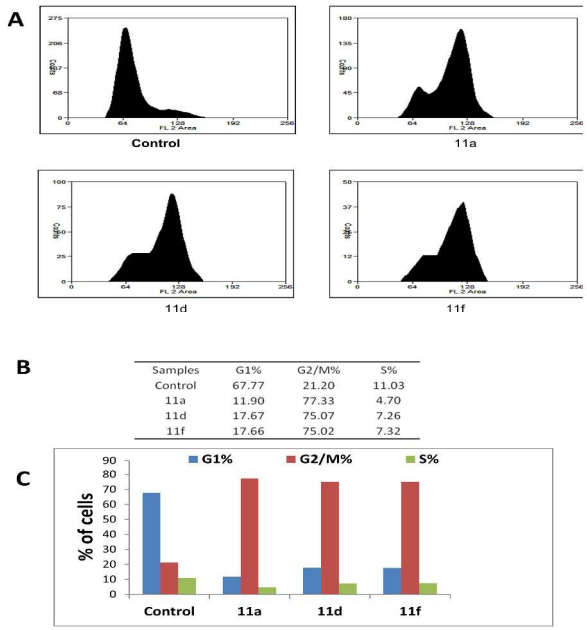

Samples	G1%	G2/M%	S%
Control	67.77	21.20	11.03
11a	11.90	77.33	4.70
11d	17.67	75.07	7.26
11f	17.66	75.02	7.32

Fig. 4 Anti-mitotic effects of 11a, 11d and **11f by FACS analysis: A.** Induction of cell cycle G2/M arrest by compounds **11a, 11d** and **11f**. A549 cells were harvested after treatment at 5 μM for 24h. Untreated cells and DMSO treated cells served as controls The percentage of cells in each phase of cell cycle was quantified by Flow Cytometry**. B.** % of the cells arrested in different stages of cell cycle by the compounds **11a**, **11d, 11f** and Control. **C.** Graphical representation of distribution of cell cycle.

were treated with **11a**, **11d** and **11f** at 5 μM concentrations for 24 h. Immunofluorescence analysis reveals that cells exhibited a rounded morphology typical of mitotic arrest population. Moreover, the chromatin was condensed in the nuclei, suggesting a metaphase arrest (Fig. 5).

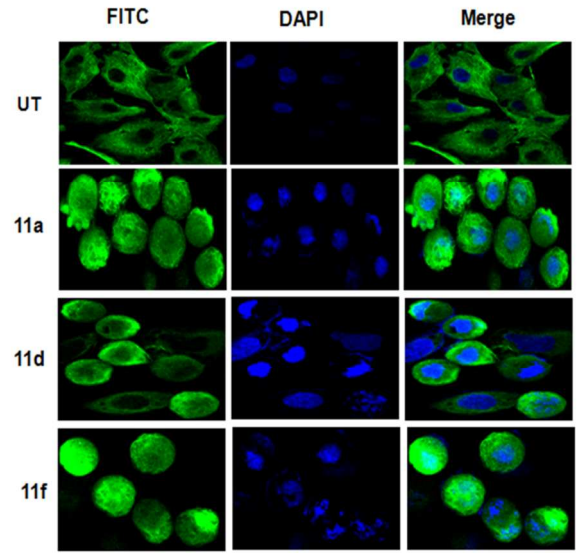

Fig. 5 Effect of 11a, 11d and 11f on microtubules and nuclear condensation. A549 cells were independently treated with **11a, 11d** and **11f** at 5 μM for 24 h. Following treatment, cells were fixed and stained for tubulin using DAPI as a counter stain. Photographs were taken using an Olympus confocal fluorescence microscope equipped with FITC and DAPI filter settings. Cells stained for tubulin and DAPI from the same field of views are given.

Microtubules exhibit dynamic equilibrium with free tubulin monomers in the cells. Pharmacological agents exploit this property of microtubules to exert their anticancer effects[28]. Since these conjugates disrupt tubulin polymerization, we elucidated their effect on cytosolic tubulin. Thus, A549 cells were treated with 5 μM concentrations of **11a**, **11d** and **11f** for 24 h. CA-4 and colchicines were also treated in the same experiment as standard reference. Subsequently, these soluble and polymerized fractions were collected and subjected to western blot analysis. Immunoblot results show that the cells exposed to these conjugates **11a**, **11d**, **11f** contain more tubulin in the soluble fraction of cells, when compared to insoluble fraction. Hence, increased tubulin in soluble fraction of cells treated with pyrazole-oxadiazole conjugates corroborated well with the inhibition of tubulin polymerization and arrest of cells in G2/M phase (Fig. 6).

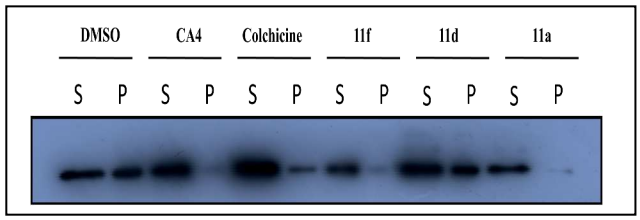

Fig. 6 Distribution of tubulin in polymerized vs soluble fractions as analyzed by immunobloting in **11a, 11d** and **11f** treated A549 cells: A549 cells were treated with 5 μM of **11a, 11d** and **11f** for 24h. CA4 and colchicine were used as positive control. Tubulin was detected by immunoblot analysis.

Effect on zebrafish development

Zebrafish (Danio rerio) has emerged as a powerful model system for chemical genetics. In order to validate these observations, we investigated the effect of lead conjugates on the development of zebrafish embryos. Therefore, embryos treated with **11a** showed remarkable delay in development as compared to DMSO treated control embryos. While the control embryos were progressing through prim6 stage, **11a** treated embryos were arrested at the 18 somite stage.[32] Embryos treated with nocodazole, also exhibited severe developmental anomalies. However, embryos treated with the conjugates **11d** and **11f** showed minimal phenotypic abnormalities. The inability of **11d** and **11f** to affect development, despite their structural similarity, suggests possible differences in the ADME (absorption, distribution, metabolism, excretion) properties of the ring substitutes *in vivo* and needs further investigation.[31-33] These observations suggest that **11a** acts as an anti-mitotic compound in zebrafish embryos and could be considered as potential chemotherpeautic lead (Fig. 7).

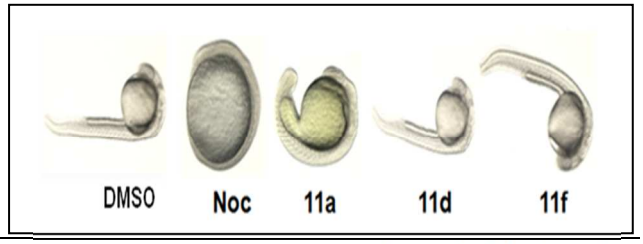

Fig. 7 Effect of microtubule inhibitors on the development of zebrafish embryos: Zebrafish embryos were treated with **DMSO, nocodazole**, **11a**, **11d** and **11f** at 5hpf. The embryos were imaged at 30hpf to observe morphological changes.

Molecular modeling

To explore possible binding modes of compounds **11a, 11d** and **11f** to tubulin, we performed molecular docking simulations on β-tubulin with tubulin cocrystal DAMA-colchicine (PDB 3E22). The computational experiments performed by employing Glide 5.8 module in Maestro 9.3 (Schrodinger suite 2012). Molecular docking analysis revealed that the three promising conjugates occupied the same position corresponding to colchicine (colchicine binding site of tubulin). Moreover, these conjugates are buried at the interface of α,β-tubulin heterodimer and the major portion is occupied in the β-subunit (showing maximum interactions) and there are fewer interactions with residues of the α-subunit (Fig. 8).[33-34] The type I conjugates functionalized with trimethoxy phenyl ring (A-ring) is an important basic unit for tubulin binding. The core structure comprising of A, B, C and D rings is sandwiched between the two subunits and surrounded by a number of amino acid residues such as N101, E183, Y202, V181, S178, G143, L248, L242, L255, K254, K352, M259, A180, A316, C241 and N249.

The docking experiments performed with individual molecules to explore the molecular interactions are depicted in Fig. 8 (**11a, 11d** and **11f**). Specifically, the docking simulations of **11a** with trimethoxyphenyl A-ring and C4 chlorophenyl D-ring have shown important hydrogen bonding interactions with some representative amino acids. The O atom of C4 methoxy group formed a strong hydrogen bond with HN of K254 (O---HN, distance 1.9 Å). In comparison, the next C4 methoxy O of the same ring formed a strong hydrogen bond with HN of E181 (O---HN, distance 2.0 Å) and the same methoxy O showed a van der Waals interactions with N101 (O---HN, distance 3.1 Å). In addition, a strong hydrogen bonding was noticed between the N atom of pyrazole ring and HS of the important amino acid C241 (N---HS, distance 2.8 Å). Most of the residues like S178, G143, L242, K254, K352, M259, A180, N258 and N249 of both the subunits have shown hydrophobic interactions with **11a**. Interestingly, B and C rings possessing heteroatoms (oxadiazole-pyrazole) exhibited hydrophilic interactions with L248 and L255. Furthermore, the D-ring with a C4 chlorophenyl group forms a π-π interaction with Y202. The conjugates **11d** and **11f** also show similar type of interactions with the amino acid residues as **11a,** however with the varying bonding distance. Where as **11d** without any substitution on the D-ring shows slight deviation in the bonding interaction and the distances are K254 (O---HN, distance 2.0 Å), E181 (O---HN, distance 2.1 Å), N101 (O---HN, distance 3.3 Å) and C241 (N---HS, distance 3.2 Å). The docking pose of **11f** with C3, C4-dichloro phenyl D-ring represent better simulations when compared to **11d** particularly in the case of given four bonding interactions and these are K254 (O---HN, distance 1.7 Å), E181 (O---HN, distance 2.1 Å), N101 (O---HN, distance 3.5 Å) and C241 (N---HS, distance 3.8 Å) (Fig. 8). Superimposition of **11a, 11d** and **11f** further confirmed that mode of binding to tubulin was similar for these conjugates. Presence of a bulky group in the D-ring, such as monomethoxy-**11b**, dimethoxy-**11i** and trimethoxy-**11h** groups do not allow successful docking possibly due to steric hindrance. Thus our results suggest that the pyrazole-oxadiazole conjugates occupy the colchicine binding pocket of tubulin and exhibit strong hydrogen bonds with the surrounding amino acids.[35]

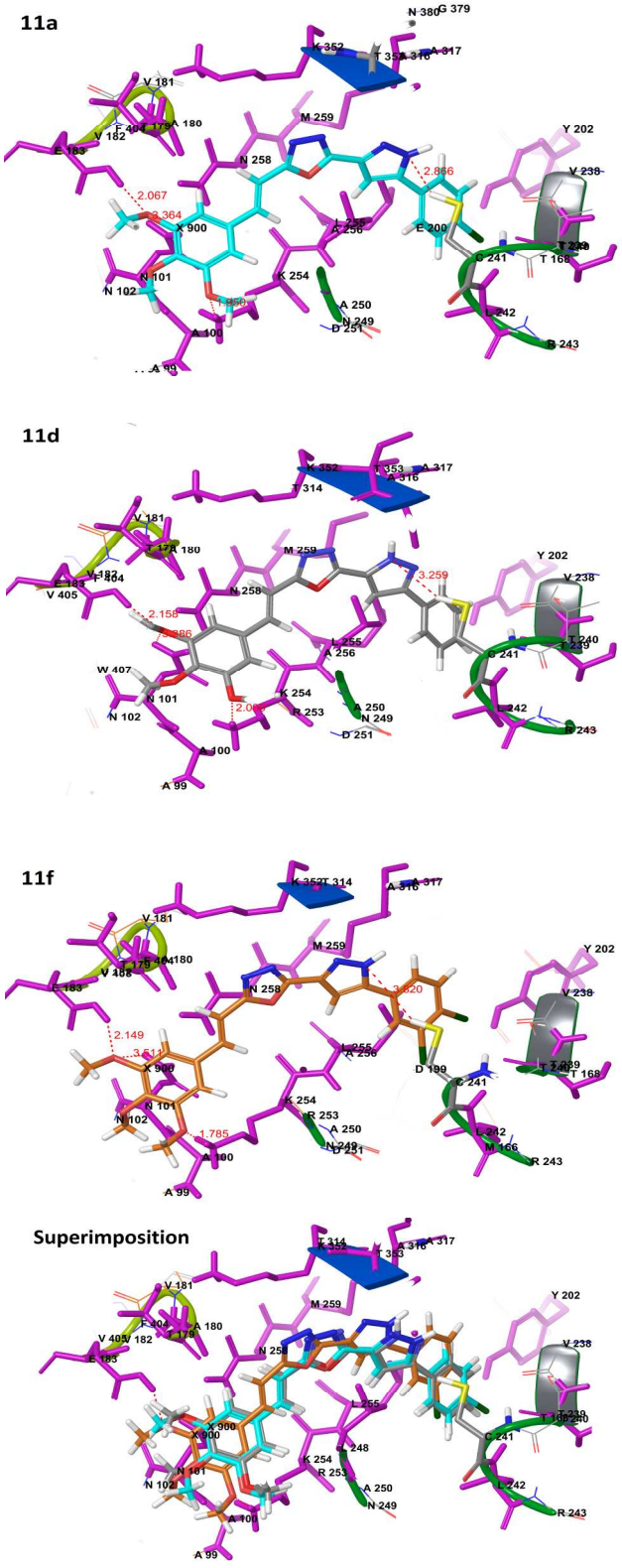

Fig. 8 Docking simulations of lead conjugates in the colchicine binding site of tubulin: 11a (light blue color)**, 11d (**grey color**)** and **11f**

(orange color) showed in stick model. The O atom of trimethoxy phenyl ring formed a strong hydrogen bond with K254, N101 and E183. The pyrazole N formed a hydrogen bond with C241. Red dotted lines indicate the hydrogen bonds and the distance was measeared indicated in red numerical. The superimposition docking pose of representative conjugates **11a 11d** and **11f** in the colchicine binding pocket. Stick representation of selected amino acids (pink color) of tubulin surrounded by the compound **11a, 11d** and **11f.**

Conclusions

In conclusion, we synthesized new class of pyrazoleoxadiazole conjugates comprising of a four ring scaffold. In order to present a comprehensive relationship between structure and activity, we prepared compounds of two structural classes. The conjugates were functionalized with four substituents at A and D rings. Most of the conjugates exhibited potential antiproliferative activity on different cancer cell lines. The presence of a monochloro or dichloro group in the D ring was essential for high antitubulin activity. The compounds **11a, 11d** and **11f** accumalation of cells in G2/M phase, induce cyclin-B1 protein and prevent chromosomal separation. Increased levels of tubulin in the soluble fraction of cells remarkably corroborated with inhibition of tubulin polymerization of these compounds. Furthermore, the lead conjugate **11a** treated with Zebrafish embryos exhibit severe developmental defects. Molecular docking studies revealed that these compounds successfully dock in the colchicine binding site of tubulin. Therefore, these results suggest that pyrazole-oxadiazole conjugates are potential inhibitors of tubulin polymerization. Finally, these conjugates are amenable for further structural modifications and could serve as useful pharmacophore templates for the generation of molecules as potential anticancer agents.

Experimental Section

Chemistry

All the chemicals and reagents were obtained from Aldrich (Sigma–Aldrich, St. Louis, MO, USA), Lancaster (Alfa Aesar, Johnson Matthey Company, Ward Hill, MA, USA), or Spectrochem Pvt. Ltd. (Mumbai, India) and were used without further purification. The completion of reactions was monitored by TLC performed on silica gel glass plates containing 60 GF-254, and visualization was achieved by UV light or iodine indicator. Column chromatography was performed with Merck 60–120 mesh silica gel. NMR spectra were recorded on Bruker UXNMR/XWIN-NMR (300 MHz) or Inova Varian-VXR-unity (400, 500 MHz) instruments. Chemical shifts (d) are reported in ppm downfield from an internal TMS standard. ESI spectra were recorded on a Micro mass Quattro LC using ESI+ software with capillary voltage 3.98 kV and ESI mode positive ion trap detector. High-resolution mass spectra (HRMS) were recorded on a QSTAR XL Hybrid MS–MS mass spectrometer. Melting points were determined with an Electro thermal melting point apparatus, and are uncorrected.

Preparation of ethyl 2,4-dioxo-4-(substituted phenyl)butanoates 8a-i

Initially sodium ethanolate was prepared in situ and diethyl oxalate (1.0 mol) was added slowly at 0 °C. The stirring was continued for 15 minutes followed by the addition of different acetophenones **7(a-i)** (1.0 mol) slowly in small portions maintaining the temperature 0 °C. After completion of addition, the stirring was continued for 4 h at room temperature. Progress of the reaction was monitored by TLC using ethylacetate and hexane as a mobile phase. After completion of reaction, neutralized by using dilute H_2SO_4 solution and further extracted with ethyl acetate followed by evaporation of the solvent under reduced pressure to obtained solid products **8(a-i)** (yield 80-90%). These were taken as such for the next step without purification

Preparation of ethyl 3-substituted phenyl-1H-pyrazole-5-carboxylates 9a-i

To each of the ethyl 2,4-dioxo-4-(substituted phenyl)butanoate **8(a-i)** (1.0 mol) produced in the previous step was added Hydrazine dihydrochloride ($N_2H_4.2HCl$) (1.5 mol) in ethanol and refluxed for 3-4 h. After completion of reaction the ethanol was removed under reduced pressure then added 150-200 mL amount of water to the residue followed by extraction with ethyl acetate (50 ml X 4). The organic layer was dried on anhydrous Na_2SO_4 and solvent was removed to obtain crude compound that was further purified by column chromatography using ethyl acetate and hexane solvent system (3:7). The pure compounds **9(a-i)** were eluted at 30-40% of ethyl acetate with good yields.

ethyl 3-(4-chlorophenyl)-1H-pyrazole-5-carboxylate 9a

Pale yellow colored solid; (yield 80.0%): R_f = 0.3 (25% ethyl acetate/hexane); ^{1}H NMR (300 MHz, $CDCl_3$); δ 1.34-1.42 (t, 3H, J_1 = 6.9 Hz, J_2 = 7.9 Hz, -C**H**$_3$), 4.33-4.41 (q, 2H, J_1 = 6.9 Hz, J_2 = 7.9 Hz, C**H**$_2$), 7.04 (s, 1H, Ar**H**), 7.36 (d, 2H, J = 7.9 Hz, Ar**H**), 7.70 (d, 2H, J = 7.9 Hz, Ar**H**) ppm; MS (ESI) *m/z* 251[M+H].

ethyl3-(4-methoxyphenyl)-1H-pyrazole-5-carboxylate 9b

Pale yellow colored solid; (yield 80.0%): R_f = 0.3 (30% ethyl acetate/hexane); ^{1}H NMR (300 MHz, $CDCl_3$); δ 1.22-1.36 (t, 3H, J_1 = 7.5Hz, -C**H**$_3$), 3.81 (s, 3H, -OC**H**$_3$), 4.20-4.35 (q, 2H, J_1 = 4.5Hz, -C**H**$_2$), 6.88-6.90 (m, 3H, Ar**H**), 7.60 (d, 2H, J = 9.0 Hz Ar**H**), 8.33 (brs, 1H, -N**H**) ppm; MS (ESI) *m/z* 248[M+H].

ethyl3-(3,4-difluorophenyl)-1H-pyrazole-5-carboxylate 9c

Yellow colored solid; (yield 75.0%): R_f = 0.3 (20% ethyl acetate/hexane); ^{1}H NMR (200 MHz, $CDCl_3$); δ 1.22-1.32 (t, 3H, J_1=7.1Hz, J_2=7.5Hz, -C**H**$_3$), 4.20-4.33 (q, 2H, J=7.1Hz, -C**H**$_2$), 7.02 (s, 1H, Ar**H**), 7.22-7.43 (m, 2H, Ar**H**), 7.72 (d, 1H, J = 6.7 Hz, Ar**H**), 9.31 (brs, 1H, -N**H**) ppm; MS (ESI) *m/z* 253[M+H].

ethyl 3-phenyl-1H-pyrazole-5-carboxylate 9d

Pale yellow colored solid; (yield 85.0%): R_f = 0.3 (25% ethyl acetate/hexane); ^{1}H NMR (500MHz, $CDCl_3$); δ 1.35-1.40 (t, 3H, J_1=6.9 Hz, -C**H**$_3$), 4.32-4.41 (q, 2H, J_1=6.9 Hz, J_2=7.9 Hz, -C**H**$_2$), 7.04 (s, 1H, Ar**H**), 7.36 (d, 2H, J = 7.9 Hz, Ar**H**) 7.36 (d, 3H, J = 7.9 Hz, Ar**H**), 9.31 (brs, 1H, -N**H**) ppm; MS (ESI) *m/z* 217[M+H].

ethyl 3-(3,4-dichlorophenyl)-1H-pyrazole-5-arboxylate 9e

yellow colored solid; (yield 75.0%): R_f = 0.3 (20% ethyl acetate/hexane); ^{1}H NMR (300 MHz, $CDCl_3$); δ 1.39-1.45 (t, 3H, *J* = 6.5 Hz, -C**H**$_3$), 4.33-4.46 (q, 2H, *J* = 7.4 Hz, -C**H**$_2$), 7.16 (s, 1H, Ar**H**), 7.49-7.63 (m, 2H, Ar**H**), 7.90-7.94 (m, 1H, Ar**H**) 8.20 (brs, 1H, -N**H**) ppm; MS (ESI) *m/z* 285 [M+H].

ethyl3-(3,4-dimethylphenyl)-1H-pyrazole-5-arboxylate 9f

yellow colored solid; (yield 80.0%): R_f = 0.3 (25% ethyl acetate/hexane); ^{1}H NMR (200 MHz, $CDCl_3$); δ 1.22-1.32 (t, 3H, *J* = 5.8 Hz, -C**H**$_3$), 2.25 (s, 6H, -C**H**$_3$), 4.17-4.30 (q, 2H, *J* = 5.8 Hz, -C**H**$_2$), 6.93 (s, 1H, Ar**H**) 7.07 (d, 1H, *J* = 8.1 Hz, Ar**H**), 7.39 (d, 1H, *J* = 6.9 Hz, Ar**H**), 7.47 (s, 1H, Ar**H**), 8.20 (brs, 1H, -N**H**) ppm; MS (ESI) *m/z* 245[M+H].

ethyl 3-(benzo[d][1,3]dioxol-5-yl)-1H-pyrazole-5-carboxylate 9g

Pale yellow colored solid; (yield 85.0%): R_f = 0.3 (40% ethyl acetate/hexane); ^{1}H NMR (400 MHz, $CDCl_3$); δ 1.35-1.42 (t, 3H, *J* = 7.5 Hz, -C**H**$_3$), 4.35-4.45 (q, 2H, *J* = 6.7 Hz, -C**H**$_2$), 6.0 (s, 2H, OC**H**$_2$O), 6.84 (d, 1H, *J* = 8.3 Hz, Ar**H**), 6.99 (s, 1H, Ar**H**), 7.21-7.26 (m, 2H, Ar**H**) ppm; MS (ESI) *m/z* 261[M+H].

ethyl 3-(3,4,5-trimethoxyphenyl)-1H-pyrazole-5-arboxylate 9h

Yellow colored solid; (yield 80.0%): R_f = 0.3 (40% ethyl acetate/hexane); ^{1}H NMR (300 MHz, $CDCl_3$); δ 1.34-1.39 (t, 3H, *J* = 7.4 Hz, -C**H**$_3$), 3.87 (s, 3H, -OC**H**$_3$), 3.88 (s, 6H, -OC**H**$_3$), 4.33-4.45 (q, 2H, J_1= 7.4 Hz, -C**H**$_2$), 7.00 (s, 2H, Ar**H**), 7.04 (s, 1H, Ar**H**) ppm; MS (ESI) *m/z* 307[M+H].

ethyl 3-(3,4-dimethoxyphenyl)-1H-pyrazole-5-carboxylate 9i

Pale yellow colored solid; (yield 80.0%): R_f = 0.3 (30% ethyl acetate/hexane); ^{1}H NMR (300 MHz, $CDCl_3$); δ 1.23-1.31 (t, 3H, *J* = 7.1 Hz, -C**H**$_3$), 3.85 (s, 3H, -OC**H**$_3$), 3.90 (s, 3H, -OC**H**$_3$), 4.19-4.32 (q, 2H, *J* = 7.1 Hz, -C**H**$_2$), 6.88 (d, 1H, J_1=7.1 Hz, Ar**H**), 6.94 (s, 1H, Ar**H**), 7.21-7.28 (m, 1H, Ar**H**) 7.29-7.34 (m, 1H, Ar**H**) 9.67 (brs, 1H, -N**H**) ppm; MS (ESI) *m/z* 277[M+H].

Preparation of 3-substituted phenyl-1H-pyrazole-5-carbohydrazides 10a-i

To the ethyl 3-substituted phenyl-1H-pyrazole-5-carboxylates **9(a-i)** obtained in the above step was added Hydrazine hydrate (4.0 mol) in ethanol at room temperature and heated to reflux for 3-4 h. The progress of reaction was monitored by TLC using ethyl acetate and hexane (1:1) as solvent system. The reaction mixture was allowed to attain room temperature and then solvent was distilled off under reduced pressure. Then residue was dissolved in water and extracted twice with ethyl acetate, dried over anhydrous Na_2SO_4 and the solvent was removed under reduced pressure to afford the corresponding compound **10** (**a-i**) as crystalline solid. The carbohydrazides obtained in this method were pure and as such taken for the next step without further purification.

Preparation of (E)-2-(3-subatituted phenyl-1H-pyrazol-5-yl)-5-(3,4,5-trimethoxystyryl)-1,3,4-oxadiazole 11a-i

To each of the 3-substituted phenyl-1H-pyrazole-5-carbohydrazides **10 (a-i)** (1.0 mol) produced in the above step was added (E)-3-(3,4,5-trimethoxyphenyl)acrylic acid (1.0 mol) in $POCl_3$ and stirred at a temperature of 110 °C for 6 h. The completion of reaction was monitored by TLC in ethyl acetate and hexane solvent system and then added ice cold water to the reaction mixture followed by extracted with ethyl acetate (50 ml X 4). The organic layer so obtained was washed with saturated $NaHCO_3$ solution and dried on anhydrous Na_2SO_4. Ethyl acetate was distilled off under vacuum to produce crude compound and this was purified by column chromatography using ethyl acetate and hexane resulted pure compounds of (E)-2-(3-subatituted phenyl-1H-pyrazol-5-yl)-5-(3,4,5-trimethoxystyryl)-1,3,4-oxadiazole **11(a-i)** in good yields (60-70%).

(E)-2-(3-(4-chlorophenyl)-1H-pyrazol-5-yl)-5-(3,4,5-trimethoxystyryl)-1,3,4-oxadiazole 11a

This compound was prepared using the procedure described above by the addition of 3-(4-chlorophenyl)-1H-pyrazole-5-carbohydrazide **10a** (236 mg 1.0 mmol) and (E)-3-(3,4,5-trimethoxyphenyl)acrylic acid (238 mg 1.0 mmol). The compound obtained as yellow colored solid Yield: 300 mg (68.4%); mp: 225-227 °C; ^{1}H NMR (300 MHz, DMSO-d_6); δ 3.79 (s, 3H, -OC**H**$_3$), 3.90 (s, 6H, -OC**H**$_3$), 6.94 (s, 2H, Ar**H**), 7.18 (d, 1H, *J* = 18.3 Hz -trans **H**), 7.45 (d, 2H, *J* = 8.4 Hz, Ar**H**), 7.59 (d, 1H, *J* = 16.2 Hz, -trans **H**), 7.79 (d, 2H, *J* = 8.4 Hz, Ar**H**), 7.90 (s, 1H, Ar**H**); ^{13}C NMR (75 MHz, DMSO-d_6): δ 54.1, 58.2, 101.3, 103.4, 107.2, 125.2, 127.1, 128.4, 131.5, 137.2, 151.2, 161.8 ppm; IR (KBr) (ν_{max}/cm^{-1}): ν = 3428, 2925, 2846, 1611, 1582, 1503, 1456, 1311, 1251, 1176, 1125, 1029,1003 cm^{-1}; MS (ESI) 439[M+H] m/z [M+H]; HR-MS (ESI) m/z for $C_{22}H_{20}N_4O_4Cl$ calculated m/z:439.11676, found m/z: 439.11597.

(E)-2-(3-(4-methoxyphenyl)-1H-pyrazol-5-yl)-5-(3,4,5-trimethoxystyryl)-1,3,4-oxadiazole 11b

This compound was prepared using the procedure described above by the addition of 3-(4-methoxyphenyl)-1H-pyrazole-5-carbohydrazide **10b** (232 mg 1.0 mmol) and (E)-3-(3,4,5-trimethoxyphenyl)acrylic acid (238 mg 1.0 mmol). The compound obtained as pale yellow colored solid Yield: 298 mg (68%); mp: 189-192 °C; ^{1}H NMR (300 MHz, DMSO-d_6); δ 3.56 (s, 3H, -OC**H**$_3$), 3.88 (s, 3H, -OC**H**$_3$), 3.94 (s, 6H, -OC**H**$_3$), 6.49 (s, 1H, Ar**H**), 6.96 (s, 1H, Ar**H**), 7.01-7.05 (m, 2H, Ar**H**), 7.11 (s, 1H, Ar**H**), 7.71 (d, 1H, *J* = 15.8 Hz, -trans**H**) 7.95-7.99 (m, 2H, Ar**H**), 8.42 (d, 1H, *J* = 15.8 Hz, -trans**H**); ^{13}C NMR (75 MHz, DMSO-d_6): δ 55.3, 55.8, 97.6, 104.9, 114.4, 120.9, 122.4, 122.9, 133.3, 128.3, 132.8, 155.8, 161.2 ppm; IR (KBr) (ν_{max}/cm^{-1}): ν = 3208, 3160, 2932, 2841, 1625, 1582, 1530, 1509, 1418, 1362, 1241, 1133, 1091, 1052 cm^{-1}; MS (ESI) *m/z* 435 [M+H]; HR-MS (ESI) *m/z* for $C_{23}H_{23}N_4O_5$ calculated *m/z*: 435.16630, found *m/z*: 435.16665.

(E)-2-(3-(3,4-difluorophenyl)-1H-pyrazol-5-yl)-5-(3,4,5-trimethoxystyryl)-1,3,4-oxadiazole 11c

This compound was prepared using the procedure described above by the addition of 3-(3,4-difluorophenyl)-1H-pyrazole-5-carbohydrazide **10c** (238 mg 1.0 mmol) and (E)-3-(3,4,5-trimethoxyphenyl)acrylic acid (238 mg 1.0 mmol). The compound obtained as brown colored solid Yield: 295 mg (67%); mp: 150-152 °C; ^{1}H NMR (300 MHz, DMSO-d_6); δ 3.81 (s, 3H, -OC**H**$_3$), 3.92 (s, 6H, -OC**H**$_3$), 6.91 (s, 2H, Ar**H**), 7.09-7.42 (m, 1H, Ar**H**), 7.21 (d, 1H, *J* = 16.0 Hz, -trans**H**), 7.52-7.73 (m, 1H, Ar**H**), 7.62 (d, 1H, *J* = 16.0 Hz, -trans**H**), 7.75-7.88 (m, 1H, Ar**H**) 7.96 (s, 1H, Ar**H**); ^{13}C NMR (75 MHz, DMSO-d_6): 54.1, 58.1, 101.6, 103.3, 103.4, 107.2, 107.4, 112.7, 112.8, 116.2, 128.3, 137.0, 137.2,151.2, 161.4, 161.7 δ ppm; IR (KBr) (ν_{max}/cm^{-1}): ν

= 3112, 3049, 2942, 1648, 1612, 1583, 1468, 1419, 1335, 1236, 1156, 1040 cm^{-1}; MS (ESI) *m/z* 441 [M+H]; HR-MS (ESI) *m/z* for $C_{22}H_{19}N_4O_4F_2$ calculated *m/z*: 441.13689, found *m/z*: 441.13681.

(E)-2-(3-phenyl-1H-pyrazol-5-yl)-5-(3,4,5-trimethoxystyryl)-1,3,4-oxadiazole 11d

This compound was prepared using the procedure described above by the addition of 3-phenyl-1H-pyrazole-5-carbohydrazide **10d** (202 mg 1.0 mmol) and (E)-3-(3,4,5-trimethoxyphenyl)acrylic acid (238 mg 1.0 mmol). The compound obtained as pale yellow colored solid Yield: 270 mg (66.8%); mp: 205-207 °C; ^{1}H NMR (300 MHz, DMSO-d_6); δ 3.86 (s, 3H, -OC**H**$_3$), 3.93 (s, 6H, -OC**H**$_3$), 6.89 (s, 2H, Ar**H**), 7.10 (d, 1H, *J* = 16.2 Hz, -trans**H**), 7.20 (s, 1H, Ar**H**), 7.40 (d, 1H, *J* = 7.1 Hz, Ar**H**), 7.43-7.52 (t, 1H, *J* = 7.5 Hz, Ar**H**), 7.63 (d, 1H, *J* = 16.4 Hz, -trans**H**), 7.67-7.71 (m, 1H, Ar**H**), 7.80 (d, 2H, *J* = 7.1 Hz, Ar**H**); ^{13}C NMR (75 MHz, DMSO-d_6): δ 55.7, 59.9, 102.4, 104.8, 108.8, 125.2, 128.2, 128.6, 130.0, 138.6, 138.9, 152.91, 158.8, 163.3 ppm; IR (KBr) (ν_{max}/cm^{-1}): ν = 3427, 3150, 3110, 3013, 2851, 1644, 1603, 1521, 1447, 1233, 1035 cm^{-1}; MS (ESI) *m/z* 405 [M+H]; HR-MS (ESI) *m/z* for $C_{22}H_{20}N_4O_4$ calculated *m/z*: 405.15573, found *m/z*: 405.15483.

(E)-2-(3-(3,4-dimethylphenyl)-1H-pyrazol-5-yl)-5-(3,4,5-trimethoxystyryl)-1,3,4-oxadiazole 11e

This compound was prepared using the procedure described above by the addition of 3-(3,4-dimethylphenyl)-1H-pyrazole-5-carbohydrazide **11e** (230 mg 1.0 mmol) and (E)-3-(3,4,5-trimethoxyphenyl)acrylic acid (238 mg 1.0 mmol). The compound obtained as pale yellow colored solid Yield: 280 mg (64.8%); mp: 222-224 °C; ^{1}H NMR (300 MHz, DMSO-d_6); δ 2.29 (s, 6H, -C**H**$_3$), 2.33 (s, 6H, -C**H**$_3$), 3.80 (s, 3H, -OC**H**$_3$), 3.92 (s, 6H, -OC**H**$_3$), 6.90 (s, 3H, Ar**H**), 6.96 (d, 2H, *J* = 5.4 Hz, Ar**H**), 7.08 (d, 1H, *J* = 16.2 Hz, -trans H), 7.12-7.26 (m, 1H, Ar**H**), 7.45 (d, 1H, *J* = 16.2 Hz, -trans H), 7.48-7.67 (m, 2H, ArH) ^{13}C NMR (75 MHz, DMSO-d_6): δ 19.1, 19.3, 55.7, 59.9, 101.8,104.8, 109.0, 109.1, 122.6, 126.3, 129.7, 130.0, 138.0, 138.6, 152.8, 163.0 ppm; IR (KBr) (ν_{max}/cm^{-1}): ν = 3143, 3000, 2938, 2835, 1647, 1583, 1528, 1504, 1451, 1419, 1333, 1244, 1186, 1154, 1125, 1038 cm^{-1}; MS (ESI) *m/z* 434 [M+H]; HR-MS (ESI) *m/z* for $C_{24}H_{25}N_4O_4$ calculated *m/z*: 433.18703, found *m/z*: 433.18632.

(E)-2-(3-(3,4-dichlorophenyl)-1H-pyrazol-5-yl)-5-(3,4,5-trimethoxystyryl)-1,3,4-oxadiazole 11f

This compound was prepared using the procedure described above by the addition of 3-(3,4-dichlorophenyl)-1H-pyrazole-5-carbohydrazide **10f** (271 mg 1.0 mmol) and (E)-3-(3,4,5-trimethoxyphenyl)acrylic acid (238 mg 1.0 mmol). The compound obtained as brown colored solid Yield: 315 mg (66.5%); mp: 158-160 °C; ^{1}H NMR (400 MHz, DMSO-d_6); δ 3.89 (s, 3H, -OC**H**$_3$), 3.90 (s, 6H, -OC**H**$_3$), 6.76 (s, 2H, Ar**H**), 6.80 (s, 1H, Ar**H**), 6.93 (d, 1H, *J* = 15.8 Hz, -trans**H**), 6.98 (d, 1H, *J* = 7.1 Hz, Ar**H**), 7.26 (s, 1H, Ar**H**), 7.40 (d, 1H, *J* = 15.8 Hz, -trans**H**), 7.52 (d, 1H, *J* = 8.2 Hz, Ar**H**); ^{13}C NMR (75 MHz, DMSO-d_6): δ 54.1, 58.2, 103.2, 107.5, 128.4, 136.3, 137.0, 137.1, 137.3, 151.2, 160.9, 161.4, 162.1 ppm; IR (KBr) (ν_{max}/cm^{-1}): ν = 3049, 3000, 2939, 2835, 1647, 1583, 1529, 1503, 1466, 1419, 1334, 1245, 1186, 1125, 1045 cm^{-1}; MS (ESI) *m/z* 511 [M+K].

(E)-2-(3-(benzo[d][1,3]dioxol-5-yl)-1H-pyrazol-5-yl)-5-(3,4,5-trimethoxystyryl)-1,3,4-oxadiazole 11g

This compound was prepared using the procedure described above by the addition of 3-(benzo[d][1,3]dioxol-5-yl)-1H-pyrazole-5-carbohydrazide **10g** (246 mg 1.0 mmol) and (E)-3-(3,4,5-trimethoxyphenyl)acrylic acid (238 mg 1.0 mmol). The compound obtained as brown red colored solid Yield: 294 mg (65.6%); mp: 199-202 °C; ^{1}H NMR (300 MHz, DMSO-d_6); δ 3.84 (s, 3H, -OC**H**$_3$), 3.94 (s, 6H, -OC**H**$_3$), 6.05 (s, 2H, -OC**H**$_2$O-), 6.86 (d, 1H, *J* = 7.9 Hz, Ar**H**), 6.94 (d, 1H, *J* = 16.8 Hz, -trans**H**), 7.09 (s, 2H, Ar**H**), 7.16 (d, 2H, *J* = 8.9 Hz, Ar**H**), 7.60 (d, 1H, *J* = 15.8 Hz, -trans**H**), 7.67-7.69 (m, 1H, Ar**H**); ^{13}C NMR (75 MHz, DMSO-d_6): δ 55.8, 60.0, 101.2, 102.0, 104.8, 105.7, 108.5, 109.2, 119.3, 130.1, 138.1, 138.8, 147.5, 147.8, 153.0, 162.6 ppm; IR (KBr) (ν_{max}/cm^{-1}): ν = 3050, 2983, 1645, 1583, 1529, 1504, 1461, 1418, 1334, 1240, 1188, 1125, 1035 cm^{-1}; MS (ESI) *m/z* 449 [M+H]; HR-MS (ESI) *m/z* for $C_{23}H_{21}N_4O_6$ calculated *m/z*:449.14556, found *m/z*: 449.14569.

(E)-2-(3-(3,4,5-trimethoxyphenyl)-1H-pyrazol-5-yl)-5-(3,4,5-trimethoxystyryl)-1,3,4-oxadiazole 11h

This compound was prepared using the procedure described above by the addition of 3-(3,4,5-trimethoxyphenyl)-1H-pyrazole-5-carbohydrazide **11h** (292 mg 1.0 mmol) and (E)-3-(3,4,5-trimethoxyphenyl)acrylic acid (238 mg 1.0 mmol). The compound obtained as yellow colored crystal Yield: 345 mg (69.8%); mp: 184-185 °C; ^{1}H NMR (400MHz, DMSO-d_6); δ 3.70 (s, 9H, -OC**H**$_3$), 3.85 (s, 9H, -OC**H**$_3$), 7.08-7.25 (m, 4H, Ar**H**), 7.37-7.50 (m, 2H, *J* = 16.9 Hz, trans**H,** Ar**H**), 7.63 (d, 1H, *J* = 16.3 Hz, trans**H,**); ^{13}C NMR (75 MHz, DMSO-d_6): δ 56.0, 60.0, 103.0, 105.4, 109.2, 124.0, 130.2, 137.7, 138.9, 153.1, 153.3, 159.1, 163.6 ppm; IR (KBr) (ν_{max}/cm^{-1}): ν = 3115, 2947, 2832, 1683, 1612, 1587, 1545, 1463, 1427, 1377, 1346, 1237, 1132, 1070 cm^{-1}; MS (ESI) *m/z* 495 [M+H]; HR-MS (ESI) *m/z* for $C_{25}H_{27}N_4O_7$ calculated *m/z*: 495.18944, found *m/z*: 495.18350.

(E)-2-(3-(3,4-dimethoxyphenyl)-1H-pyrazol-5-yl)-5-(3,4,5-trimethoxystyryl)-1,3,4-oxadiazole 11i

This compound was prepared using the procedure described above by the addition of 3-(3,4-dimethoxyphenyl)-1H-pyrazole-5-carbohydrazide **10i** (262 mg 1.0 mmol) and (E)-3-(3,4,5-trimethoxyphenyl)acrylic acid (238 mg 1.0 mmol). The compound obtained as brown colored solid Yield: 315 mg (67.8%); mp: 158-160 °C; ^{1}H NMR (300 MHz, DMSO-d_6); δ 3.89 (s, 3H, -OC**H**$_3$), 3.91 (s, 9H, -OC**H**$_3$), 3.93 (s, 3H, -OC**H**$_3$), 6.76 (s, 1H, Ar**H**), 6.80 (d, 2H, *J* = 6.2 Hz, Ar**H**), 6.92 (d, 1H, *J* = 16.3 Hz, -trans**H**), 6.98 (d, 1H, *J* = 16.3 Hz, -trans**H**), 7.04-7.08 (m, 1H, Ar**H**), 7.19-7.25 (m, 1H Ar**H**), 7.39-7.45 (m, 1H Ar**H**); ^{13}C NMR (75 MHz, DMSO-d_6): δ 55.9, 60.0, 105.2, 109.3, 130.2, 138.1, 138.8, 153.0, 162.9, 163.9 ppm; IR (KBr) (ν_{max}/cm^{-1}): ν = 3150, 2883, 1660, 1645, 1553, 1529, 1500, 1461, 1418, 1287, 1240, 1188, 1125, 1033 cm^{-1}; MS (ESI) *m/z* 465 [M+H].

Preparation of (E)-2-(2-(benzo[d][1,3]dioxol-5-yl)vinyl)-5-(3-substituted phenyl-1H-pyrazol-5-yl)-1,3,4-oxadiazole 12 a-i

To each of the 3-substituted phenyl-1H-pyrazole-5-carbohydrazides **10(b-i)** (1.0 mol) produced in the above step was added (E)-3-(benzo[d][1,3]dioxol-5-yl)acrylic acid (1.0 mol) in $POCl_3$ and stirred at a temperature of 110 °C for 5 h. The completion of reaction was monitored by TLC in ethyl acetate and hexane solvent system and then added ice cold water to the

reaction mixture followed by extracted with ethyl acetate (50 ml X 4). The organic layer so obtained was washed with saturated $NaHCO_3$ solution and dried on anhydrous Na_2SO_4. Ethyl acetate was distilled off under vacuum to produce crude compound and this was further purified by column chromatography using ethyl acetate and hexane afforded pure compounds of each (E)-2-(2-(benzo[d][1,3]dioxol-5-yl)vinyl)-5-(3-substituted phenyl-1H-pyrazol-5-yl)-1,3,4-oxadiazole12 (**a-i**) in good yields (65-75%).

(E)-2-(2-(benzo[d][1,3]dioxol-5-yl)vinyl)-5-(3-(4-chlorophenyl)-1H-pyrazol-5-yl)-1,3,4-oxadiazole 12a

This compound was prepared using the procedure described above by the addition of 3-(4-chlorophenyl)-1H-pyrazole-5-carbohydrazide **10a** (236 mg 1.0 mmol) and (E)-3-(benzo[d][1,3]dioxol-5-yl)acrylic acid (192 mg 1.0 mmol). The compound obtained as brown colored solid Yield: 263 mg (67%); mp: 164-166 °C; ^{1}H NMR (300 MHz, DMSO-d_6); δ 6.04 (s, 2H, -OC**H**$_2$O-), 6.81 (d, 1H, *J* = 16.4 Hz, -trans**H**), 6.84 (d, 2H, *J* = 7.7 Hz, Ar**H**), 7.0 (d, 1H, *J* = 8.1 Hz, Ar**H**), 7.09-7.21 (m, 2H, Ar**H**), 7.41 (d, 1H, *J* = 16.4 Hz, -trans**H**), 7.46 (s, 2H, Ar**H**), 7.64-7.84 (m, 1H, Ar**H**); ^{13}C NMR (75 MHz, DMSO-d_6): δ 101.4, 106.0, 108.0, 108.3, 124.0, 129.0, 137.8, 147.9, 148.6, 162.8, 163.9 ppm; IR (KBr) (ν_{max}/cm^{-1}): ν = 2924, 2854, 1743, 1638, 1603, 1579, 1530, 1496, 1445, 1355, 1316, 1255, 1255, 1227, 1097, 1033, 965 cm^{-1}; MS (ESI) *m/z* 393 [M+H].

(E)-2-(2-(benzo[d][1,3]dioxol-5-yl)vinyl)-5-(3-(4-methoxyphenyl)-1H-pyrazol-5-yl)-1,3,4-oxadiazole 12b

This compound was prepared using the procedure described above by the addition of 3-(4-methoxyphenyl)-1H-pyrazole-5-carbohydrazide **10b** (232 mg 1.0 mmol) and (E)-3-(benzo[d][1,3]dioxol-5-yl)acrylic acid (192 mg 1.0 mmol). The compound obtained as yellow colored solid Yield: 235 mg (65.6%); mp: 186-189 °C; ^{1}H NMR (500 MHz, DMSO-d_6); δ 3.81 (s, 3H, -OC**H**$_3$) 6.09 (s, 2H, -OC**H**$_2$O-), 6.98 (d, 1H, *J* = 7.9 Hz, Ar**H**), 7.02 (d, 2H, *J* = 7.7 Hz, Ar**H**), 7.16-7.40 (m, 3H, *J* = 15.2 Hz, -trans**H,** Ar**H**), 7.53 (s, 1H, Ar**H**), 7.60 (d, 1H, *J* = 16.4 Hz, -trans**H**), 7.81 (d, 2H, *J* = 7.7 Hz, Ar**H**); ^{13}C NMR (75 MHz, DMSO-d_6): δ 55.2, 101.4, 101.8, 106.1, 106.2, 107.8, 108.4, 114.4, 120.7, 124.2, 126.8, 129.1, 137.5, 138.5, 143.9, 148.0, 148.8, 159.2, 159.5, 163.6 ppm; IR (KBr) (ν_{max}/cm^{-1}): ν = 3195, 2922, 2852, 1608, 1501, 1447, 1257, 1360, 1308, 1177, 1119, 1032, 965 cm^{-1}; MS (ESI) *m/z* 389 [M+H]; HR-MS (ESI) *m/z* for $C_{21}H_{17}N_4O_4$ calculated *m/z*: 389.12443, found *m/z*: 389.12518.

(E)-2-(2-(benzo[d][1,3]dioxol-5-yl)vinyl)-5-(3-(3,4-difluorophenyl)-1H-pyrazol-5-yl)-1,3,4-oxadiazole 12c

This compound was prepared using the procedure described above by the addition of 3-(3,4-difluorophenyl)-1H-pyrazole-5-carbohydrazide **10c** (238 mg 1.0 mmol) and (E)-3-(benzo[d][1,3]dioxol-5-yl)acrylic acid (192 mg 1.0 mmol). The compound obtained as yellow colored solid yield: 250 mg (63.4%); mp: 210-212 °C; ^{1}H NMR (300 MHz, DMSO-d_6); δ 6.04 (s, 2H, -OC**H**$_2$O-), 6.88 (s, 1H, Ar**H**), 6.99 (d, 1H, *J* = 16.6 Hz, -trans**H**), 7.09 (s, 1H, Ar**H**), 7.23 (s, 1H, Ar**H**), 7.42-7.68 (m, 1H, Ar**H**), 7.59 (d, 1H, *J* = 16.4 Hz, -trans**H**), 7.72-7.84 (m, 1H, Ar**H**), 7.88 (s, 2H, Ar**H**), 13.93 (brs, 1H, -NH); ^{13}C NMR (75 MHz, DMSO-d_6): δ 101.4, 103.6, 106.1, 107.7, 108.4, 114.5, 117.3, 118.4, 122.3, 123.4, 124.3, 129.0, 138.7, 139.7, 148.0, 148.9, 163.7 ppm; IR (KBr) (ν_{max}/cm^{-1}): ν = 3116, 3055, 2921, 2853, 1637, 1609, 1503, 1494, 1491, 1446, 1362, 1246, 1036 cm^{-1}; MS (ESI) *m/z* 395[M+H]; HR-MS (ESI) *m/z* for $C_{20}H_{13}F_2N_4O_3$ calculated *m/z*:395.09502, found *m/z*: 395.09491.

(E)-2-(2-(benzo[d][1,3]dioxol-5-yl)vinyl)-5-(3-phenyl-1H-pyrazol-5-yl)-1,3,4-oxadiazole 12d

This compound was prepared using the procedure described above by the addition of 3-phenyl-1H-pyrazole-5-carbohydrazide **10d** (202 mg 1.0 mmol) and (E)-3-(benzo[d][1,3]dioxol-5-yl)acrylic acid (192 mg 1.0 mmol). The compound obtained as saffron colored solid Yield: 235 mg (65.5%); mp: 220-222 °C; ^{1}H NMR (400 MHz, DMSO-d_6); δ 6.04 (s, 2H, -OC**H**$_2$O-), 6.87 (d, 1H, *J* = 8.1 Hz, Ar**H**), 6.92 (d, 1H, *J* = 16.2 Hz, -trans**H**), 7.05-7.11 (m, 2H, Ar**H**), 7.20 (s, 1H, Ar**H**), 7.35-7.48 (m, 4H, Ar**H**), 7.61 (d, 1H, *J* = 16.4 Hz, -trans**H**), 7.77 (d, 1H, *J* = 7.1 Hz, Ar**H**); ^{13}C NMR (75 MHz, DMSO-d_6): δ 101.5, 102.8, 106.2, 107.7, 108.4, 124.3, 125.4, 128.7, 129.0, 129.1, 138.6, 148.0, 148.8, 163.7 ppm; IR (KBr) (ν_{max}/cm^{-1}): ν = 3448, 3120, 3069, 2995, 2956, 2828, 1677, 1610, 1516, 1337, 1247, 1207, 1167, cm^{-1}; MS (ESI) *m/z* 359 [M+H]; HR-MS (ESI) *m/z* for $C_{20}H_{15}N_4O_3$ calculated *m/z*: 359.11387, found *m/z*: 359.11377.

(E)-2-(2-(benzo[d][1,3]dioxol-5-yl)vinyl)-5-(3-(3,4-dimethylphenyl)-1H-pyrazol-5-yl)-1,3,4-oxadiazole 12e

This compound was prepared using the procedure described above by the addition of 3-(3,4-dimethylphenyl)-1H-pyrazole-5-carbohydrazide **10e** (230 mg 1.0 mmol) and (E)-3-(benzo[d][1,3]dioxol-5-yl)acrylic acid (192 mg 1.0 mmol). The compound obtained as pale yellow colored solid Yield: 265 mg (68.6%); mp: 187-189 °C; ^{1}H NMR (400 MHz, DMSO-d_6); δ 2.28 (s, 3H, -CH$_3$), 2.32 (s, 3H, -CH$_3$), 6.08 (s, 2H, -OC**H**$_2$O-), 6.91 (s, 1H, Ar**H**), 7.07-7.32 (m, 4H, *J* = 16.0 Hz, -trans**H,** Ar**H**), 7.40 (s, 1H, Ar**H**), 7.58 (d, 3H, *J* = 16.0 Hz, -trans**H,** Ar**H**); ^{13}C NMR (75 MHz, DMSO-d_6): δ 19.0, 19.2,101.1, 101.8, 105.7, 108.0, 122.5, 123.5, 126.2, 128.7, 129.6, 136.5, 136.6, 138.2, 147.9, 148.7, 163.3 ppm; IR (KBr) (ν_{max}/cm^{-1}): ν = 3170, 3068, 2918, 2851, 1663, 1522, 1498, 1485, 1418, 1360, 1253, 1169, 1031 cm^{-1}; MS (ESI) *m/z* 387 [M+H]; HR-MS (ESI) *m/z* for $C_{22}H_{19}N_4O_3$ calculated *m/z*: 387.14517, found *m/z*: 387.14565.

(E)-2-(2-(benzo[d][1,3]dioxol-5-yl)vinyl)-5-(3-(3,4-dichlorophenyl)-1H-pyrazol-5-yl)-1,3,4-oxadiazole 12f

This compound was prepared using the procedure described above by the addition of 3-(3,4-dichlorophenyl)-1H-pyrazole-5-carbohydrazide **10f** (271 mg 1.0 mmol) and (E)-3-(benzo[d][1,3]dioxol-5-yl)acrylic acid (192 mg 1.0 mmol). The compound obtained as yellow colored solid Yield: 285 mg (66.7%); mp: 186-188 °C; ^{1}H NMR (400 MHz, DMSO-d_6); δ 6.01 (s, 2H, -OC**H**$_2$O-), 6.82-6.86 (m, 1H, ArH), 6.82 (d, 1H, *J* = 16.0 Hz, -trans**H**), 6.99 (d, 1H, *J* = 8.0 Hz, Ar**H**), 7.05 (s, 2H, Ar**H**), 7.26 (s, 3H, Ar**H**), 7.40 (d, 1H, *J* = 16.0 Hz, -trans**H**); ^{13}C NMR (75 MHz, DMSO-d_6): δ 101.4, 106.0, 108.0, 108.3, 124.0, 129.0, 137.8, 148.6, 147.9, 162.8, 163.9 ppm; IR (KBr) (ν_{max}/cm^{-1}): ν = 3421, 2916, 1652, 1635, 1604, 1559, 1499, 1447, 1318, 1256, 1228, 1102, 1036 cm^{-1}; MS (ESI) *m/z* 427 [M+H]; HR-MS (ESI) *m/z* for $C_{20}H_{13}Cl_2N_4O_3$ calculated *m/z*: 427.03592, found *m/z*: 427.03582.

(Z)-5-methoxy-3-((3-(3,4,5-trimethoxyphenyl)-1H-pyrazol-5-yl)methylene)indolin-2-one 12g

This compound was prepared using the procedure described above by the addition of 3-(benzo[d][1,3]dioxol-5-yl)-1H-pyrazole-5-carbohydrazide **10g** (246 mg 1.0 mmol) and (E)-3-

(benzo[d][1,3]dioxol-5-yl)acrylic acid (192 mg 1.0 mmol). The compound obtained as saffron colored solid yield: 270 mg (67%); mp: 196-198 °C; ^{1}H NMR (300 MHz, DMSO-d_6); δ 6.01 (s, 4H, OCH2O), 6.53 (d, 1H, *J* = 15.5 Hz, -trans**H**), 6.81 (d, 2H, *J* = 7.7 Hz, Ar**H**), 7.0 (d, 1H, *J* = 7.7 Hz, Ar**H**), 7.05 (s, 1H, Ar**H**), 7.45-7.63 (m, 4H, *J* = 15.5 Hz, -trans**H**, Ar**H**); ^{13}C NMR (75 MHz, DMSO-d_6): δ 101.4, 106.2, 108.5, 117.4, 123.5, 128.9, 139.8, 147.9, 148.6, 163.8,167.7 ppm; IR (KBr) (ν_{max}/cm^{-1}): ν = 3198, 3020, 1637, 1601, 1483, 1443, 1365, 1251, 1101, 1037 cm^{-1}; MS (ESI) *m/z* 403 [M+H].

(E)-2-(2-(benzo[d][1,3]dioxol-5-yl)vinyl)-5-(3-(3,4,5-trimethoxyphenyl)-1H-pyrazol-5-yl)-1,3,4-oxadiazole 12h

This compound was prepared using the procedure described above by the addition of 3-(3,4,5-trimethoxyphenyl)-1H-pyrazole-5-carbohydrazide **11h** (292 mg 1.0 mmol) and (E)-3-(benzo[d][1,3]dioxol-5-yl)acrylic acid (192 mg 1.0 mmol). The compound obtained as light yellow colored solid Yield: 300 mg (66.9%); mp: 228-230 °C; ^{1}H NMR (300 MHz, DMSO-d_6); δ 3.84 (s, 3H, -OC**H**$_3$), 3.94 (s, 6H, -OC**H**$_3$), 6.05 (s, 2H, -OC**H**$_2$O-), 6.86 (d, 1H, *J* = 7.9 Hz, Ar**H**), 6.94 (d, 1H, *J* = 16.8 Hz, -trans**H**), 7.09 (s, 2H, Ar**H**), 7.16 (d, 1H, *J* = 8.9 Hz, Ar**H**), 7.60 (d, 1H, *J* = 15.8 Hz, -trans**H**), 7.67-7.69 (m, 1H, Ar**H**); ^{13}C NMR (75 MHz, DMSO-d_6): δ 54.3, 58.5, 99.8, 101.0, 101.3, 104.3, 106.0, 106.7, 122.2, 127.4, 136.2, 136.8, 146.5, 147.3, 151.6, 161.9 ppm; IR (KBr) (ν_{max}/cm^{-1}): ν = 3136, 3103, 2924, 1638, 1589, 1527, 1503, 1490, 1468, 1253, 1123, 1036 cm^{-1}; MS (ESI) *m/z* 449 [M+H]; HR-MS (ESI) *m/z* for $C_{23}H_{21}N_4O_6$ calculated *m/z*: 449.14556, found *m/z*: 449.14424.

(E)-2-(2-(benzo[d][1,3]dioxol-5-yl)vinyl)-5-(3-(3,4-dimethoxyphenyl)-1H-pyrazol-5-yl)-1,3,4-oxadiazole 12i

This compound was prepared using the procedure described above by the addition of 3-(3,4-dimethoxyphenyl)-1H-pyrazole-5-carbohydrazide **10i** (262 mg 1.0 mmol) and (E)-3-(benzo[d][1,3]dioxol-5-yl)acrylic acid (192 mg 1.0 mmol). The compound obtained as light yellow colored solid Yield: 265 mg (63.3%); mp: 172-174 °C; ^{1}H NMR (500 MHz, DMSO-d_6); δ 3.78 (s, 3H, -OC**H**$_3$), 3.85 (s, 3H, -OC**H**$_3$), 6.09 (s, 2H, -OC**H**$_2$O-), 6.99 (s, 1H, Ar**H**), 7.02 (s, 1H, Ar**H**), 7.13-7.31 (m, 2H, Ar**H**), 7.36 (s, 1H, Ar**H**), 7.45 (d, 2H, *J* = 16.7 Hz, -trans**H**) 7.36 (s, 1H, Ar**H**), 7.45 (d, 1H, *J* = 16.7 Hz, -trans**H**); ^{13}C NMR (75 MHz, DMSO-d_6): δ 55.6, 59.7, 101.5, 102.2, 106.2, 107.8, 108.5, 109.2, 112.0, 117.9, 121.2, 124.3, 129.1, 138.6, 149.0, 149.1, 159.0, 163.6 ppm; IR (KBr) (ν_{max}/cm^{-1}): ν = 3117, 2917, 1684, 1620, 1549, 1515, 1461, 1416, 1337, 1244, 1187, 1127, 1079, 1039 cm^{-1}; MS (ESI) *m/z* 419 [M+H]; HR-MS (ESI) *m/z* for $C_{22}H_{19}N_4O_5$ calculated *m/z*: 419.13500, found *m/z*: 419.13453.

Preparation of ethyl 2,4-dioxopentanoate 14

Initially sodium ethanolate was prepared insitu and diethyl oxalate (1.0 mol) was added slowly at 0 °C. Continued the stirring for 15 minutes followed by added acetone **(13)** (1.0 mol) drop wise maintaining the temperature 0 °C. After completion of addition the stirring was continued for 4 h at room temperature. The reaction mixture was neutralized by the addition of dilute H_2SO_4 solution and further extracted with ethyl acetate to obtain product **14** (yield 80-90%) which was taken as such for the next step without purification.

Preparation of ethyl 3-methyl-1H-pyrazole-5-carboxylate 15

The produced ethyl 2,4-dioxopentanoate (**14**) (1.0 mol) were added to Hydrazine dihydrochloride (N_2H_4.2HCl) (1.5 mol) in ethanol and refluxed for 3-4 h. Progress of the reaction was monitored by TLC using ethylacetate-hexane solvent system. The ethanol was distilled under vacuum then added water to the residue followed by extracted with ethyl acetate (50 ml X 4). The organic layer was dried on anhydrous Na_2SO_4 and evaporated the solvent to obtain crude compound that was further purified by column chromatography using ethyl acetate and hexane solvent system. The pure compound **(15)** was eluted at 25-30% of ethyl acetate with good yields. Yellow colored solid; (yield 80.0%): R_f = 0.3 (30% ethyl acetate/hexane); ^{1}H NMR (300 MHz, $CDCl_3$); δ 1.32-1.41 (t, 3H, *J* = 6.7 Hz, -C**H**$_3$), 2.36 (s, 3H, -C**H**$_2$), 4.32-4.44 (q, 2H, J_1= 6.7 Hz, J_1= 7.5 Hz, -C**H**$_2$), 7.04 (s, 1H, Ar**H**) ppm; MS (ESI) *m/z* 155 [M+H].

Preparation of 3-methyl-1H-pyrazole-5-carbohydrazide 16

To the ethyl 3-methyl-1H-pyrazole-5-carboxylate **(15)** obtained in the above step was added Hydrazine hydrate (4.0 mol) in ethanol at room temperature and then heated to reflux for 3-4 h. The completion of reaction was monitored by TLC using ethyl acetate and hexane (1:1) system. The reaction mixture was allowed to attain room temperature and then solvent was distilled off under reduced pressure. The residue was dissolved in water and extracted twice with ethyl acetate, dried over anhydrous Na_2SO_4 and the solvent was removed under reduced pressure to afford the compound (**16**) as crystalline solid. The carbohydrazide obtained in this method was pure and as such taken for the next step without further purification.

(E)-2-(3-methyl-1H-pyrazol-5-yl)-5-(3,4,5-trimethoxystyryl)-1,3,4-oxadiazole17a

To the 3-methyl-1H-pyrazole-5-carbohydrazide **16** (154 mg 1.0 mol) produced in the above step was added (E)-3-(3,4,5-trimethoxyphenyl)acrylic acid (238 mg 1.0 mol) in $POCl_3$ and stirred at a temperature of 110 °C for 6 h. The completion of reaction was monitored by TLC in ethyl acetate and hexane solvent system and then added ice cold water to the reaction mixture followed by extracted with ethyl acetate (50 ml X 4). The organic layer so obtained was washed with saturated $NaHCO_3$ solution and dried on anhydrous Na_2SO_4. Ethyl acetate was distilled off under vacuum to produce crude compound and this was further purified by column chromatography using ethyl acetate and hexane yielded yellow colored pure compound of (E)-2-(3-methyl-1H-pyrazol-5-yl)-5-(3,4,5-trimethoxystyryl)-1,3,4-oxadiazole (**17a**) in good yield: 240 mg (70%); mp: 15-152 °C; ^{1}H NMR (400 MHz, DMSO-d_6); δ 2.57 (s, 3H, -C**H**$_3$), 3.85 (s, 3H, -OC**H**$_3$), 3.89 (s, 6H, -OC**H**$_3$), 6.71 (s, 2H, Ar**H**), 6.76 (s, 1H, Ar**H**), 6.86 (d, 1H, *J* = 16.8 Hz, -trans**H**), 7.36 (d, 1H, *J* = 15.8 Hz, -trans**H**); ^{13}C NMR (75 MHz, DMSO-d_6): δ 8.9, 54.2, 58.4, 103.2, 107.6, 128.5, 136.5, 137.1, 137.3, 137.5, 151.4, 160.9, 161.6, 162.3 ppm; IR (KBr) (ν_{max}/cm^{-1}): ν = 3503, 3049, 2999, 2940, 2834, 1641, 1583, 1503, 1466, 1334,1245, 1125 cm^{-1}; MS (ESI) *m/z* 343 [M+H].

(E)-2-(2-(benzo[d][1,3]dioxol-5-yl)vinyl)-5-(3-methyl-1H-pyrazol-5-yl)-1,3,4-oxadiazole 17b

To the 3-methyl-1H-pyrazole-5-carbohydrazide **16** (154 mg, 1.0 mol) produced in the above step was added (E)-3-(benzo[d][1,3]dioxol-5-yl)acrylic acid (192 mg 1.0 mmol) in $POCl_3$ and stirred at a temperature of 110 °C for 5 h. The completion of reaction was monitored by TLC in ethyl acetate and hexane solvent system and then added ice cold water to the reaction mixture followed by extracted with ethyl acetate (50 ml X 4). The organic layer so obtained was washed with saturated $NaHCO_3$ solution and dried on anhydrous Na_2SO_4. Ethyl acetate was distilled off under vacuum to produce crude compound and this was further purified by column chromatography using ethyl acetate and hexane afforded pale yellow colored pure compound of (E)-2-(2-(benzo[d][1,3]dioxol-5-yl)vinyl)-5-(3-methyl-1H-pyrazol-5-yl)-1,3,4-oxadiazole (**17b**) in good yield: 200 mg (67.5%); mp: 210-212 °C; ^{1}H NMR (400 MHz, DMSO-d_6); δ 2.55 (s, 3H, -C**H**$_3$), 5.99 (s, 2H, -OC**H**$_2$O), 6.74 (d, 1H, *J* = 8.0 Hz, Ar**H**), 6.79 (s, 1H, Ar**H**), 6.95 (d, 1H, *J* = 8.0 Hz, Ar**H**), 7.04 (d, 1H, *J* = 16.0 Hz, -trans**H**), 7.24 (s, 1H, Ar**H**), 7.35 (d, 1H, *J* = 16.0 Hz, -trans**H**); ^{13}C NMR (75 MHz, DMSO-d_6): δ 8.7, 99.5, 104.1, 106.4, 106.6, 122.0, 127.2, 135.9, 146.1, 146.8, 160.8, 162.1 ppm; IR (KBr) (ν_{max}/cm^{-1}): ν = 3448, 3120, 3069, 2995, 2956, 2828, 1677, 1610, 1516, 1337, 1247, 1207, 1167 cm^{-1}; MS (ESI) *m/z* 297 [M+H].

Biology

Cell cultures, maintenance and antiproliferative evaluation

All the cell lines used in this study were purchased from the American Type Culture Collection (ATCC, United States). A549, MCF-7, HeLa and IMR32 were grown in Dulbecco's modified Eagle's medium (containing 10% FBS in a humidified atmosphere of 5% CO2 at 37 °C). Cells were trypsinized when sub-confluent from T25 flasks/60 mm dishes and seeded in 96-wel plates. The pyrazole-oxadiazole conjugates were evaluated for their in vitro antiproliferative in four different human cancer cell lines. A protocol of 48 h continuous drug exposure was used and a SRB cell proliferation assay was employed to estimate cell viability or growth. The cell lines were grown in their respective media containing 10% fetal bovine serum and were seeded into 96-well microtiter plates in 200 µL aliquots at plating densities depending on the doubling time of individual cell lines. The microtiter plates were incubated at 37 °C, 5% CO2, 95% air, and 100% relative humidity for 24 h prior to addition of experimental drugs. Aliquots of 2 µL of the test compounds were added to the wells already containing 198 µL of cells, resulting in the required final drug concentrations. For each compound, four concentrations (0.1, 1, 10 and 100 µM) were evaluated, and each was done in triplicate wells. Plates were incubated further for 48 h, and the assay was terminated by the addition of 100 µL of 10% (wt/vol) cold trichloroacetic acid and incubated at 4 °C for 1 h. The supernatant was discarded. The plate was washed four times with tap water and was allowed to air dry. The cells were then stained with 0.057% SRB dissolved in 1% acetic acid for 30 min at room temperature. Unbound SRB was washed away with four washes of 1% acetic acid. The plate was again allowed to air dry and the bound SRB stain, representing surviving cells, was dissolved in 50 μL of Tris base (10 mM). The optical density was determined at 510 nm using a microplate reader (Enspire,Perkin Elmer, USA). Percent growth was calculated on a plate by plate basis for test wells relative to control wells. The above determinations were repeated thrice. The growth inhibitory effects of the compounds were analyzed by generating dose response curves as a plot of the percentage surviving cells versus compound concentration. The sensitivity of the cancer cells to the test compound was expressed in terms of IC_{50}, a value defined as the concentration of compound that produced 50% reduction as compared to the control absorbance. IC_{50} values are indicated as means ± SD of three independent experiments [25c].

Dot-blot assay

A549 cells were treated with 5 µM concentrations of (**11a-i**, **12a-i** and **17a-b**) for 24 h. Subsequently, cells were harvested and proteins were quantified using Amido Black followed by densitomerty analysis. Equal amount of protein were blotted on nitrocellulose membrane using Bio-Dot SF microfiltration apparatus (Bio-Rad). Briefly, nitrocellulose membrane and 3 filters papers (Whatmann 3) were soaked in IX TBS solution for 10 min. Later, the filter papers, membrane were arranged in the apparatus and connected to vacuum pump (Millipore). The membranes were rehydrated using 100 µl of 1XTBS by vacuum filtration. Subsequently, 50 µl volumes of samples were blotted on the membranes and washed with 200 µl of 1X TBS through application of vacuum. The blot was blocked with 5% blotto for 1 h at room temperature. Immunoblot analysis was performed as described previously using UVP, biospectrum 810 imaging system.[25c]

Tubulin polymerization assay

An *in vitro* assay for monitoring the time-dependent polymerization of tubulin to microtubules was performed employing a fluorescence-based tubulin polymerization assay kit (BK011, Cytoskeleton, Inc.) according to the manufacturer's protocol. The reaction mixture in a final volume of 10 µl in PEM buffer (80 mM PIPES, 0.5 mM EGTA, 2 mM $MgCl_2$, pH 6.9) in 384 well plates contained 2 mg/mL bovine brain tubulin, 10 µM fluorescent reporter, 1 mM GTP in the presence or absence of test compounds at 37^{o}C. Tubulin polymerization was followed by monitoring the fluorescence enhancement due to the incorporation of a fluorescence reporter into microtubules as polymerization proceeds. Fluorescence emission at 420 nm (excitation wavelength is 360 nm) was measured for 1 h at 1-min intervals in a multimode plate reader (Tecan M200). To determine the IC_{50} values of the compounds against tubulin polymerization, the compounds were pre-incubated with tubulin at varying concentrations (0.001, 0.01, 0.1, 1, 10 and 100 µM). Assays performed under similar conditions as employed for polymerization assays as described above. [27]

Analysis of cell cycle

A549 cells in 60 mm dishes were incubated for 24 h in the presence or absence of test compounds **11a**, **11d** and **11f** at 5 μM concentration. Cells were harvested with Trypsin-EDTA, fixed with ice-cold 70% ethanol at 4^{o}C for 30 min, ethanol was removed by centrifugation and cells were stained with 1 mL of DNA staining solution [0.2 mg of Propidium Iodide (PI), and 2 mg RNase A] for 30 min as described earlier . The DNA contents of 20,000 events were measured by flow cytometer (BD FACSCanto II). Histograms were analyzed using FCS express 4 plus.[29]

Immunohistochemistry of tubulin and analysis of nuclear morphology

A549 cells were seeded on glass cover slip, incubated for 24 h in the presence or absence of test compounds **11a**, **11d** and **11f** at a concentration of 5 μM. Cells grown on cover slips were fixed in 3.5% formaldehyde in phosphate-buffered saline (PBS) pH 7.4 for 10 minutes at room temperature. Cells were permeabilized for 6 minutes in PBS containing 0.5% Triton X-100 (Sigma) and 0.05% Tween-20 (Sigma). The permeabilized cells were blocked with 2% BSA (Sigma) in PBS for 1h. Later, the cells were incubated with primary antibody for tubulin from (sigma) at (1:200) diluted in blocking solution for 4h at room temperature. Subsequently the antibodies were removed and the cells were washed thrice with PBS. Cells were then incubated with FITC labeled anti-mouse secondary antibody (1:500) for 1h at room temperature. Cells were washed thrice with PBS and mounted in medium containing DAPI. Images were captured using the Olympus confocal microscope FLOW VIEW FV 1000 series and analyzed with FV10ASW 1.7 series software.

Western blot analysis of soluble versus polymerized tubulin

Cells were seeded in 12-well plates at 1×10^5 cells per well in complete growth medium. Following treatment of cells with respective compounds (**11a**, **11d** and **11f)** for duration of 24 h, cells were washed with PBS and subsequently soluble and insoluble tubulin fractions were collected. To collect the soluble tubulin fractions, cells were permeabilized with 200 μL of pre-warmed lysis buffer [80 mM Pipes-KOH (pH 6.8), 1 mM $MgCl_2$, 1 mM EGTA, 0.2% Triton X-100, 10% glycerol, 0.1% protease inhibitor cocktail (Sigma-Aldrich)] and incubated for 3 min at 30 ^oC. Lysis buffer was gently removed, and mixed with 100 μL of 3×Laemmli's sample buffer (180 mM Tris-Cl pH 6.8, 6% SDS, 15% glycerol, 7.5% β-mercaptoethanol and 0.01% bromophenol blue). Samples were immediately heated to 95 ^oC for 3 min. To collect the insoluble tubulin fraction, 300 μL of 1×Laemmli's sample buffer was added to the remaining cells in each well, and the samples were heated to 95^oC for 3 min. Equal volumes of samples were run on an SDS-10 % polyacrylamide gel and were transferred to a nitrocellulose membrane employing semidry transfer at 50 mA for 1h. Blots were probed with mouse anti-human α-tubulin diluted 1:2,000 ml (Sigma) and stained with rabbit anti-mouse secondary antibody coupled with horseradish peroxidase, diluted 1:5000 ml (Sigma). Bands were visualized using an enhanced Chemiluminescence protocol (Pierce) and radiographic film (Kodak).

Zebrafish screening

Wild type zebrafish (Danio rerio) were raised and maintained at 28.5^oC with 14hr:10 hr light : dark cycle. 2-3 pairs of zebrafish were synchronously mated and embryos were pooled. The embryos were dechlorinated and 3-4 embryos were dispensed in 200 μl of E3 embryo medium (5 mM NaCl, 0.17 mM KCl, 0.44 mM $CaCl_2$ and 0.68 mM $MgCl_2$) into each well of a 96 well plate. The embryos were treated with the compound **11a, 11d** and **11f** (10 & 25 μM), nocodazole (5 μM) or DMSO (1%) at 5hpf and incubated at 28.5^oC. About 20 embryos were screened for each compound in biological replicates. They were observed after 28hpf with a Leica steromicroscope. Only those compounds that resulted in similar phenotypic defects in most of the embryos were considered as active.[29]

Molecular modeling

Glide 5.8 module in Maestro 9.3 (Schrodinger suite 2012) was employed to dock pyrazole-oxadiazole conjugates in colchicine binding site of tubulin.[30] The structure of the compounds were drawn by using 2D sketcher and converted to 3D structure in maestro 9.3. By using LigPrep (2.5) module the drawn ligands geometry was optimized by using the Optimized Potentials for Liquid Simulations-2005 (OPLS-2005) force field. To fix the geometry of drawn conjugates, we have assigned to determine chirality from 3D structure from workspace in LigPrep. So that it generated ligand with fixed stereo centers. The crystal structure (PDB code 3E22) was obtained from the RCSB protein data bank (http://www.rcsb.org/pdb). Protein preparation wizard of Schrodinger suite has been used to prepare protein. The proteins were preprocessed separately by deleting the substrate cofactor as well as the crystallographically observed water molecules (water without H bonds), correcting the mistakes in PDB file, optimizing hydrogen bonds. After assigning charge and protonation state finally energy minimization with root mean square deviation (RMSD) value of 0.30Å was performed using OPLS2005 force field. Receptor grid was generated at active site of protein crystal structure with length of 20 A°. After completion of protein and ligand preparation, each ligand is docked in prepared protein individually. Glide XP (Extra Precision) was employed for all docking analysis and was performed in glide Flexible docking with default parameters. The best docked poses were selected as the ones with the lowest Glide Score; the more negative the Glide Score, the more favorable the binding. [31-32]

Acknowledgement

A.B.S, G.B.K and V.S.R acknowledge CSIR-UGC, New Delhi and for the award of senior research fellowship. We also acknowledge CSIR for financial support under the 12th Five Year plan project "Affordable Cancer Therapeutics (ACT)" (CSC0301) and "Small Molecules in Lead Exploration (SMiLE)" (CSC0111). We thank Dr. K. Ravinder for assistance with zebrafish assays.

Notes and references

[a]*Medicinal Chemistry and Pharmacology, CSIR – Indian Institute of Chemical Technology, Hyderabad 500 007, India; Phone: (+) 91-40-27193157; Fax: (+) 91-40-27193189; E-mail: ahmedkamal@iict.res.in*

[b]*Centre for Chemical Biology CSIR-Indian Institute of Chemical Technology Hyderabad 500 007, India*

[c]*Nuclear Magnetic Resonance Centre, CSIR-Indian Institute of Chemical Technology Hyderabad 500 007, India*

[d]*Department of Medicinal Chemistry National Institute of Pharmaceutical Education and Research (NIPER), Hyderabad-500 037, India*

[e]*CSIR – Centre for Cellular and Molecular Biology, Hyderabad–500 007, India*

†Electronic Supplementary Information (ESI) available: [^{1}H NMR and ^{13}C NMR spectra of final compounds are provided]. See DOI: 10.1039/b000000x/

1. R. Heald, E. Nogales, *J. Cell Sci.* 2002, 115, 3−4.
2. M. A. Jordan, L. Wilson, *Nat. Rev. Cancer.* 2004, **4**, 253−265.
3. J. Lowe, H. Li, K. Downing, E. Nogales, *J. Mol. Biol.* 2001, **313**, 1045−1057.
4. B. Gigant, C. Wang, R. B. G. Ravelli, F. Roussi, M. O. Steinmetz, P. A. Curmi, A. Sobel, M. Knossow, *Nature.* 2005, **435**, 519−522.

5. Z. Chen, P. J. Merta, N. H. Lin, S. K. Tahir, P. Kovar, H. L. Sham, H. Zhang. *Mol. Cancer Ther.* 2005, **4**, 562-568.
6. RD. Vale *Cell*. 2003, **112**, 467-480.
7. J. Howard, AA. Hyman, *Curr Opin Cell Biol.* 2007**, 19**, 31–35.
8. TJ. Mitchison, ED. Salmon, *Nat Cell Biol.* 2001**, E17**-21. Review. Erratum in: *Nat Cell Biol*. 2001, **3(5)**, 530.
9. Q. Li, H. L. Sham, *Expert Opin. Ther. Pat.* 2002, **12,** 1663-1702.
10. C. M. Lin, H. H. Ho, G. R. Pettit, E. Ha mel, *Biochemistry*. 1989, **28,** 6984-6991.
11. RJ. Vasquez, B. Howell, AM. Yvon, P. Wadsworth, L. Cassimeris. *Mol Biol Cell*. 1997 **8(6)**, 973-985.
12. A. Sachse, L. Penkova, G. Noel, S. Dechert, O. A. Varzatskii, I. O. Fritsky, F. Meyer, *Synthesis*. 2008, 800−806.
13. C. A. Dvorak, D. A. Rudolph, S. Ma, N. I. Carruthers, *J. Org. Chem.* 2005, **70**, 4188−4190.
14. SA. Rostom. *Bioorg Med Chem.* 2010, **18(7),** 2767-2776.
15. IV. Magedov, L. Frolova, M. Manpadi, Ud. Bhoga, H. Tang, NM. Evdokimov, O. George, KH. Georgiou, S. Renner, M. Getlik, TL. Kinnibrugh, MA. Fernandes, S. Van slambrouck, WF. Steelant, CB. Shuster, S. Rogelj, WA. van Otterlo, A. Kornienko, *J Med Chem*. 2011 **54(12),** 4234-4246.
16. B. Abu Thaher, M. Arnsmann, F. Totzke, J.E. Ehlert, M.H. Kubbutat, C. Schächtele, M.O. Zimmermann, P. Koch, F.M. Boeckler, S.A. Laufer, *J. Med. Chem*. 2012**, 55,** 961-965.
17. HZ. Zhang, S. Kasibhatla, J. Kuemmerle, W. Kemnitzer, K. Ollis-Mason, L. Qiu, C. Crogan-Grundy, B. Tseng, J. Drewe, SX. Cai. *J Med Chem.* 2005, **48(16),** 5215-5223.
18. A. Kamal, D. Dastagiri, MJ. Ramaiah, EV. Bharathi, JS. Reddy, G. Balakishan, P. Sarma, SN. Pushpavalli, M. Pal-Bhadra, A. Juvekar, S. Sen, S. Zingde. *Bioorg. Med. Chem.* 2010 **18(18),** 6666-6677.
19. L. Lee, LM. Robb, M. Lee, R. Davis, H. Mackay, S. Chavda, B. Babu, EL. O'Brien, AL. Risinger, SL. Mooberry, M. Lee. *J Med Chem.* 2010, **53(1),** 325-334.
20. M. Rashid, A. Husain, R. Mishra. *Eur. J. Med. Chem.* 2012, **54,** 855-866.
21. L. Eugene, C. Piatnitski, S. K. Alexander, O. Xiaohu, C. Xiaoling, P. Vatee, W. Ying, T. M. Carolina, F. D. Jacqueline. *ACS Med. Chem. Lett.* 2010, **1,** 488–492.
22. P. Horrocks, M. R. Pickard, H. H. Parekh, S. P. Patelb, and Ravindra B. Pathak. *Org. Biomol. Chem.* 2013*,* **11,** 4891–4898.
23. A. Kamal, G. Ramakrishna, P. Raju, A.V. Rao, A. Viswanath, V.L. Nayak, S. Ramakrishna. *Eur. J. Med. Chem.* 2011, **46,** 2427- 2435.
24. P. Singh, M. Kaur, W. Holzer, *Eur. J. Med. Chem.* 2010, **45(11),** 4968-4982.
25. a) A. Kamal, Y. V. V. Srikanth, TB. Shaik, M. Naseer A Khan, Md. Ashraf, M. Kashi Reddy, K. Anil Kumar and SV. Kalivendi, *Med. Chem. Commun.* 2011, **2,** 819-823; b) A. Kamal, AB. Shaik, G. Narender Reddy, CG. Kumar, J. Joseph, GB. Kumar, U. Purushotham, GN. Sastry. *Med. Chem. Res*. 2014, **23,** 2080–2092; c) A. Kamal, AB. Shaik, N. Jain, C. Kishore, A. Nagabhushana, B. Supriya, GB. Kumar, SS. Chourasiya, Y Suresh, RK. Mishra, A. Addlagatta 10.1016/j.ejmech.2013.10.077.
26. PS. Frisa, JW. Jacobberger. *PLoS. One.* 2009, **18,** 4(*9*), 7064.
27. A. S. Kumar, M. A. Reddy, N. Jain, C. Kishor, T.R. Murthy, D. Ramesh, B. Supriya, A. Addlagatta, S. V. Kalivendi, B. Sreedhar. *Eur. J. Med. Chem.* 2013, **60,** 305-324.
28. Minotti, A. M. Barlow, S. B. Cabral, F. *J. Biol. Chem.* 1991, **266,** 3987-3994.
29. C. Riccardi, I. Nicoletti. *Nat. Protoc.* 2006, **1(3),** 1458-1461.
30. a) Glide version 5.8, Schrödinger, LLC, New York, NY, 2012; b) Maestro, version 9.3, Schrödinger, LLC, New York, NY, 2012.
31. C. B. Kimmel, W. W. Ballard, S. R. Kimmel, B. Ullmann, T. F. Schilling. *Dev. Dyn.* 1995, **203,** 253-310.
32. RD. Murphey, HM. Stern, CT. Straub, LI. Zon. *Chem Biol Drug Des*. 2006, **68(4),** 213-219.
33. H.S. Moon, E.M. Jacobson, S.M. Khersonsky, M.R. Luzung, D.P. Walsh, W. Xiong, J.W. Lee, P.B. Parikh, J.C. Lam, T.W. Kang, G.R. Rosania, A.F. Schier, Y.T. Chang. *J. Am. Chem. Soc.* 2002, **124,** 11608-11609.
34. MA. Reddy, N. Jain, D. Yada, C. Kishore, JR. Vangala, R. P Surendra, A. Addlagatta, SV. Kalivendi, B. Sreedhar. *J* Med Chem. 2011, **54(19),** 6751-6760.
35. R. Romagnoli, PG. Baraldi, A. Brancale, A. Ricci, E. Hamel, R. Bortolozzi, G. Basso, G. Viola. J Med Chem. 2011, **54(14),** 5144-5153.

Graphical abstract

A library of pyrazole-oxadiazole conjugates were synthesized and investigated for their antiproliferative activity in human cancer cell lines. Among the conjugates **11a, 11d,** and **11f** significantly inhibited cell growth as well as tubulin polymerization. Docking simulations performed on the tubulin at colchicine binding site to determine the possible binding modes of potent conjugates.